Universidade de Aveiro
Ano 2022

Departamento de Química

Óscar Manuel Ferreira Fonseca

O papel da proteína sérica amiloide A3 na osteopenia durante a infeção por *Mycobacterium avium*

The role of Serum Amyloid A3 protein in bone loss during *Mycobacterium avium* infection

Universidade de Aveiro
Ano 2022

Departamento de Química

Óscar Manuel Ferreira Fonseca

O papel da proteína sérica amiloide A3 na osteopenia durante a infeção por *Mycobacterium avium*

The role of Serum Amyloid A3 protein in bone loss during *Mycobacterium avium* infection

Dissertação apresentada à Universidade de Aveiro para cumprimento dos requisitos necessários à obtenção do grau de Mestre em Bioquímica, realizada sob a orientação científica da Doutora Ana Cordeiro Gomes, do Instituto de Investigação e Inovação em Saúde; da Professora Doutora Maria Salomé Gomes, Professora Associada com agregação do Departamento de Biologia Molecular do Instituto de Ciências Biomédicas Abel Salazar, da Universidade do Porto, e Group Leader no Instituto de Investigação e Inovação em Saúde; e do Professor Doutor Pedro Fontes Oliveira, Professor Auxiliar do Departamento de Química da Universidade de Aveiro.

o júri

presidente

Professor Doutor Brian James Goodfellow
Professor auxiliar da Universidade de Aveiro

vogais

Arguente principal – Doutora Rita Faria Santos
Professor auxiliar convidada da Escola Superior de Saúde do Instituto Politécnico do Porto

Orientador – Doutora Ana Rita Azevedo Cordeiro Gomes
Investigadora Júnior do Instituto de Investigação e Inovação em Saúde (i3S) da Universidade do Porto

The work described on this thesis was conducted at the Host Targets of Infection group at Instituto de Biologia Molecular e Celular / Instituto de Investigação e Inovação em Saúde (IBMC/i3S).

We acknowledge the support of i3S Scientific Platforms: Advanced Light Microscopy (ALM); Animal Facility; BioSciences Screening and Cell Culture and Genotyping Core Facility. ALM and BioSciences Screening are members of the national infrastructure the Portuguese Platform of Bioimaging (PPBI-POCI-01-0145-FEDER-022122). BioSciences Screening is also a member of the national infrastructure PT-OPENSCREEN (NORTE-01-0145-FEDER-085468).

Scientific illustrations were created using BioRender.com, under a premium plan belonging to Ana Cordeiro Gomes.

This work was supported by the project “Inflammabone - Understanding how chronic infection disrupts the hematopoietic niche leading to osteopenia” (KOG-202108-00929) from the European Hematology Society (EHA).

agradecimentos

Esta tese encerra um capítulo da minha vida que não se cinge apenas a este último ano académico. Por isso, cabe-me agradecer a todos os que foram importantes, indispensáveis e que fizeram parte deste longo caminho.

Começo por agradecer à Professora Salomé Gomes, minha coorientadora durante este último ano. Agradeço-lhe ter-me permitido integrar o seu grupo de investigação, toda a disponibilidade, preocupação e a revisão desta tese.

De seguida, agradeço à Doutora Ana Cordeiro Gomes, orientadora desta tese. Primeiramente, agradeço a oportunidade que me proporcionou em observar e aprender como se faz e desenvolve ciência de qualidade excecional. De seguida, agradeço-lhe o facto de me ter sempre estimulado a desenvolver as minhas capacidades de pensamento crítico, autonomia, curiosidade científica e comunicação, entre tantas outras. Para além disto, agradeço-lhe sobretudo ter-me ensinado e sempre relembrado que a ciência não se faz de "bons" resultados, faz-se de pensamento, de ideias e de muita vontade. Ainda mais, agradeço-lhe toda a paciência que teve comigo durante este ano, toda a preocupação que sempre mostrou, a confiança que depositou em mim desde o início, as conversas para nunca baixar os braços e o facto de fazer de tudo para que tanto eu como o meu trabalho se revelassem um sucesso, para que no fim, como ela sempre diz, "possas brilhar". Obrigado por tudo.

Continuo ao agradecer ao grupo "Host Targets of Infection", os HoTIs, por me terem integrado tão bem não só no grupo de investigação, como também no grande grupo de amigos que são. À Doutora Ana Carolina Moreira, agradeço-lhe todas as vezes que se mostrou preocupada comigo, toda a sua incansável boa disposição e por me ter dado a grande e valiosa oportunidade de "subir ao comboio" neste futuro próximo. À Doutora Tânia Silva, agradeço todas as vezes que me levou a pensar nas melhores e importantes escolhas para o meu futuro, mostrando-se sempre preocupada e disponível para ajudar. Aos meus colegas de "noções", Clara e Gabriel, pela sua ajuda, por me lembrarem sempre que é preciso "relativizar a situação" e até pelos bons momentos de procrastinação, obrigado meus caros.

Não posso deixar de agradecer também ao Professor Pedro Oliveira, meu coorientador da Universidade de Aveiro, que se mostrou sempre preocupado e disponível desde o início do processo de escolha de tese, e a quem devo um agradecimento especial por me ter levado a fazer a feliz escolha que fiz. Agradeço-lhe ainda a revisão desta tese.

De seguida, agradeço a todos os incríveis amigos que Aveiro me deu, estes anos foram tão especiais maioritariamente por vocês, que família bonita. Em especial, agradeço às minhas amigas que me acompanharam neste ano de mudança, Bia, Inês S., Inês B, Isa, Clara e Lúcia, que sorte tenho em vos ter. À nova colega de casa, Margarida, por todos os momentos filosóficos de leveza que trouxe durante este ano.

Volto a agradecer à minha casa nestes últimos dois anos, à Lú e à Clara, com quem partilhei tanto, com quem cresci e com quem me senti tão feliz. Obrigado por tantos jantares em família moderna, obrigado por todos os momentos de privação excêntrica, por tantas conquistas e derrotas que vivenciámos juntos, por nos aturarmos como só uma família se atura e por terem feito com que os regressos fossem sempre melhores por saber que de casa ia para casa, obrigado favs.

Falando de amigos, deixo o meu muito obrigado aos meus de Tarouca, sobretudo a vocês Adriana, Bruna e André, por estes anos todos e por aqueles que estão para vir. Por todos os cafés de horas que passam a voar, por todos os momentos e cumplicidade que o 5252 nos trouxe, mas, sobretudo, por me mostrarem que mesmo seguindo caminhos separados, as nossas amizades caminham lado a lado, obrigado por tudo.

De seguida, agradeço à minha família, às minhas primas quase irmãs, Carina e Vitória, por todos os momentos de felicidade e por ter o privilégio de crescer ao vosso lado. Aos meus tios Sandra e Rui, por se preocuparem como pais e por se mostrarem sempre tão ou mais felizes que eu com as minhas conquistas. Aos meus avós, Manuel, Vitória e Leopoldina, que desde que me lembro têm sempre um sorriso nos lábios e me mostram o quanto gostam de mim.

Ao meu irmão, Humberto, com quem desde os meus 8 anos tenho a grande sorte de partilhar tudo. A ti, agradeço-te os abraços, sorrisos e gargalhadas. Agradeço-te por me mostrares sempre como te orgulhas de mim e por fazeres com que eu me orgulhe tanto de ti. Obrigado por me deixares e ensinares a crescer contigo, por me teres sempre mostrado como é bom manter sempre uma criança dentro de nós, por partilharmos o nosso Bigotes, por depositares em mim tanta confiança e, sobretudo, por gostares tanto de mim como eu gosto de ti.

Por fim, o meu maior agradecimento é para a minha mãe e para o meu pai, a quem devo tudo e que merecem o meu obrigado constante. Começo por agradecer-vos a melhor educação e valores que me poderiam ter dado. Agradeço-vos a vida tão feliz que sempre conseguiram proporcionar-me, à custa de todo o vosso esforço. Agradeço toda a confiança que depositam em mim, todo o orgulho que mostram e sentem, o apoio constante que me dão e por nunca, mas nunca me deixarem desistir. Mais importante ainda, obrigado por me mostrarem o afortunado que sou em ter-vos como pais, pelo amor e carinho sem fim que estão sempre prontos para dar e pelos abraços reconfortantes que me deixam sempre em casa. Mãe, Pai, obrigado por serem sempre a casa onde quero voltar, amo-vos muito.

palavras-chave

Infeção micobacteriana, remodelação óssea, TNFα, IFNγ, SAA3, osteoclastos, osteoblastos

resumo

As infeções micobacterianas podem levar à perda de massa óssea sem que ocorra colonização direta do osso. A osteopenia resultante surge de uma desregulação do processo de remodelação óssea, quer pelo aumento da degradação do osso, quer pela diminuição da sua formação. A perda de massa óssea resultante da infeção é provocada pela produção de mediadores do sistema imune pelo hospedeiro após a entrada do agente patogénico. Estudos prévios utilizando um modelo *in vivo* de infeção disseminada por *M. avium* indicaram que a diminuição da massa óssea é dependente de IFNγ e TNFα, e que o *Saa3* é o gene cuja expressão mais aumenta com a infeção nos ossos destes animais. Sendo assim, esta tese tem por objetivo aprofundar os mecanismos moleculares de perda de massa óssea associados às infeções micobacterianas e compreender o papel da proteína sérica amiloide A3 (SAA3) na degradação e formação óssea.

Aqui mostramos que macrófagos infetados por *M. avium* produzem fatores solúveis pro-osteoclastogénicos (SPOFs) como o TNFα que aumentam a reabsorção óssea pelos osteoclastos. A produção de TNFα pelos macrófagos infetados por *M. avium* é estimulada pelo IFNγ. Também demonstrámos que a SAA3 é outro SPOF produzido por macrófagos infetados por *M. avium in vitro*, e que o TNFα aumenta a expressão de *Saa3* em macrófagos infetados. Determinámos também que osteoclastos diferenciados *in vitro* produzem SAA3 quando estimulados com TNFα. Aferimos que a proteína SAA estimula a osteoclastogénese, ainda que não aumente a atividade de reabsorção destas células. Porém, a adição de TNFα aumenta a proporção de trincheiras. Além disso, aferimos também que o meio condicionado de macrófagos infetados não teve efeito na capacidade de mineralização dos osteoblastos e que a adição de SAA diminuiu-a, o que indica que a SAA prejudica a diferenciação dos osteoblastos e a sua atividade.

No geral, os nossos resultados realçam um possível mecanismo molecular para a perda de massa óssea durante uma infeção crónica, em que o IFNγ, TNFα e SAA3 são as moléculas-chave. A infeção por *M. avium* leva à produção de IFNγ, que irá instruir os macrófagos a produzirem SPOFs como o TNFα e a SAA3. A infeção crónica vai levar à destruição do osso, uma vez que a SAA e o TNFα aumentam a formação e atividade dos osteoclastos respetivamente. Simultaneamente, a proteína SAA dificulta quer a diferenciação quer a atividade dos osteoblastos. Os nossos resultados enfatizam o papel das proteínas SAA, particularmente a SAA3, como proteínas chave na remodelação óssea durante a infeção por micobactérias.

keywords

Mycobacterial infection, bone turnover, TNFα, IFNγ, SAA3, osteoclasts, osteoblasts

abstract

Mycobacterial infections can lead to the loss of bone mass without direct colonization of the bone. Osteopenia arises from a dysregulation of the bone turnover, due to enhanced bone degradation and/or impaired new bone formation. The indirect bone loss during infection is due to the production of immune mediators by the host upon pathogen invasion. Previous studies using a murine model of *M. avium* disseminated infection indicated that bone mass was decreased in an IFNγ and TNFα-dependent manner, and that *Saa3* was the gene whose expression in the bone increases the most with infection. Therefore, this thesis aims to further understand the molecular mechanisms of bone loss associated to chronic mycobacterial infection and dissect the role of the serum amyloid A3 protein (SAA3) in bone degradation and bone formation.

Here, we show that *M. avium*-infected macrophages produce soluble pro-osteoclastogenic factors (SPOFs) that increase bone resorption by osteoclasts. We identified TNFα as a SPOF produced by infected macrophages and whose production is potentiated by IFNγ. Moreover, we assessed that SAA3 is another SPOF produced by *M. avium*-infected macrophages *in vitro* and TNFα enhances *Saa3* expression in infected macrophages. Likewise, we determined that *in vitro* differentiated osteoclasts produce SAA3 upon TNFα stimulation. Furthermore, the SAA protein stimulates osteoclastogenesis, while not enhancing their resorptive activity. However, TNFα addition increases the proportion of trenches. We further found that the conditioned media from infected macrophages had no effect on the mineralization capacity of osteoblasts and that SAA diminished it, indicating that SAA impairs osteoblastic differentiation and activity.

Overall, our results highlight a possible molecular mechanism for bone loss during chronic infection, in which IFNγ, TNFα, and SAA3 are the key molecules. *M. avium* infection leads to the production of IFNγ, which will instruct macrophages to produce SPOFs like TNFα and SAA3. Chronic infection will increase bone destruction, as SAA and TNFα enhance the formation and activity of osteoclasts, respectively. Simultaneously, SAA protein impairs osteoblastic differentiation and activity. Our results emphasize the role of SAA proteins, particularly the SAA3 protein, as key proteins in the bone turnover process during mycobacterial infection.

INDEX

LIST OF ABBREVIATIONS

AG	Arabinogalactan
ATP	Adenosine triphosphate
BRC	Bone-remodeling compartment
CatK	Cathepsin K
DKK1	Dickkopf WNT Signaling Pathway Inhibitor 1
DMEM	Dulbecco's Modified Eagle's Medium
DPI	Days post-infection
EDTA	Ethylenediamine tetraacetic acid
HSC	Hematopoietic stem cells
IFNγ	Interferon gamma
IL	Interleukin
MA	Mycolic acids
MAC	*Mycobacterium avium* complex
M-CSF	Monocyte/macrophage colony-stimulating factor
MMPs	Matrix metalloproteinases
MSC	Mesenchymal stem cells
NTM	Non-tuberculous mycobacteria
OCP	Osteoclast progenitors
OPG	Osteoprotegerin
PG	Peptidoglycan
PTH	Parathyroid hormone
RANKL	Receptor activator of nuclear factor kappa-B ligand
RUNX2	RUNX Family Transcription Factor 2
SAA3	Serum Amyloid A3
SEM	Scanning electron microscopy
SEMA4D	Semaphorin 4D
S1P	Sphingosine 1-phosphate
SPOF	Soluble pro-osteoclastogenic factor
SZ	Sealing zone
TB	Tuberculosis
TNF	Tumor Necrosis Factor
TRAP	Tartrate-resistant acid phosphatase
USA	United States of America
WHO	World Health Organization

LIST OF FIGURES

INTRODUCTION

Chapter 1. The *Mycobacterium* Genus

Mycobacteria are thought to have emerged 150 million years ago, during the Jurassic era, and are now found almost in every habitat and ecosystem on the planet [1]. Bacilli-shaped mycobacteria are aerobic bacteria [2] that belong to the vast *Actinobacteria* phylum [3]. Many of these pathogens are saprophytes, whereas others are obligatory or opportunistic pathogens [2].

As mycobacteria are highly resilient to high temperatures [4], and hypoxic conditions [5], they are found in a variety of environments, including the ground, soil, tap water, animals, and humans. Indeed, their presence in water poses a significant risk to both human's and animal's health [6]. Apart from the stated sources, mycobacteria have been found in a diversity of eatables. Unpasteurized milk and dairy products such as cheeses and newborn powdered formula, meat and its products, seafood, vegetables, and fruit juices are all potential sources of mycobacterial transmission to people through food and drink [7].

Mycobacteria are Gram-positive bacteria with a high (G + C) content (62 – 70%) but are acid-fast [2]. While the increase of GC content in bacteria is related to a higher optimum temperature and a wider tolerance range [8], their acid-fast behavior allows them to resist decolorization with acid alcohol, after staining. This last significant and distinctive trait has been attributed to various components of the mycobacterial cell wall, especially the high content of mycolic acids [9, 10]. Moreover, this characteristic explains the need for specific techniques such as the Ziehl-Neelsen staining, instead of the Gram method. The use of this technique allows the distinction of infections by microorganisms that do not exhibit acid-fast behavior [9, 11]. Nevertheless, differential identification within the various species of mycobacteria is challenging and new molecular laboratory methods are required [12, 13]. The specific sequencing of genes like *rpoB* and *hsp65* has been very helpful, but above all, the use of the 16S rRNA is the one that has offered the most advances in this field of research. Furthermore, multigene sequencing or whole-genome sequencing may be useful techniques to distinguish and discover new *Mycobacterium* species [12, 13].

The exceptional molecular complexity of the mycobacterial cell wall (**Figure 1**) is a unique trait that distinguishes *Mycobacterium* species from the vast majority of other prokaryotes [14], and it is partly responsible for the mycobacteria's pathogenic success and

innate resistance [3]. The cell wall's inner structure is composed of a peptidoglycan cross-linked polymer (PG), a highly branched arabinogalactan (AG) polysaccharide, and long-chain mycolic acids (MA) [15-17], while the outer part is composed of glycolipids and lipoglycans, which interact with the MA [16, 18]. All these lipid layers are responsible for the acid-fast resistance of mycobacteria [9, 16]. The inner structure represents an insoluble complex that spreads outward in layers from the plasma membrane and influences mycobacterial species' growth, survival under stress, pathogenicity, and antibiotic resistance [6]. The early stages of the biosynthesis of these components have been underutilized as antibacterial targets to date, and so represent considerable potential for the development of new antimycobacterial drugs [14, 15, 18].

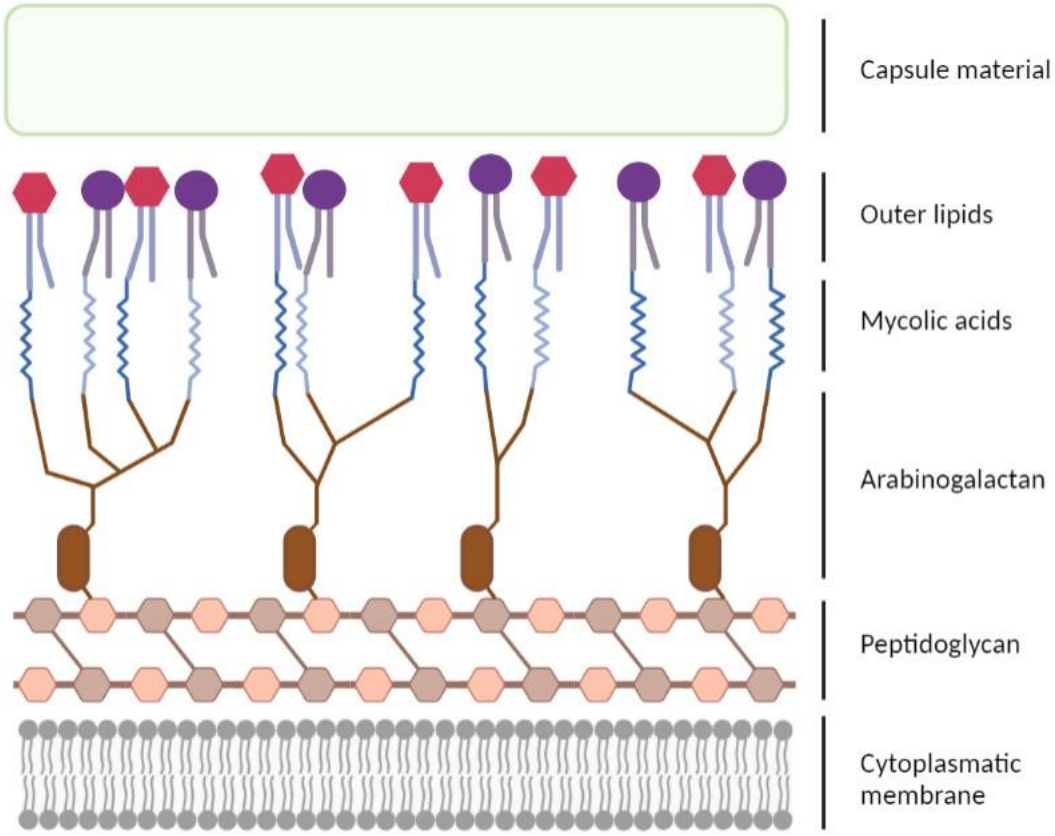

Figure 1 – **The mycobacterial cell wall.** Simplified schematic representation of the mycobacterial cell wall, depicting the noteworthy components, including peptidoglycan, arabinogalactan, mycolic acids, and the outer lipids. The lipid layers confer acid-fast behavior to the mycobacteria, while the inner structure influences their growth and resistance. Figure created using BioRender.com.

1.1. Classification of mycobacteria

There are presently 169 different species in the genus *Mycobacterium*, and many of these species have just recently been found or reclassified thanks to modern molecular identification techniques [1, 19]. Of this large number of species, some mycobacterial species are well-known human pathogens, such as *M. tuberculosis*, *M. leprae*, and *M. ulcerans* [20]. Mycobacteria may be divided into three major groups (**Figure 2**): the *M. tuberculosis complex*, *M. leprae*, and mycobacteria other than tuberculosis-causing and *M. leprae*, generally known as non-tuberculous mycobacteria (NTM). The NTM species may also be categorized as being true pathogens, like *M. ulcerans*; opportunistic pathogens, which includes the ones belonging to the *Mycobacterium avium* complex; or saprophytes, such as *Mycobacterium smegmatis*. Mycobacteria can be categorized further based on their rate of growth; fast-growing species (less than 7 days to form visible colonies in culture) are frequently non-pathogenic, whereas slow-growing species (more than 7 days to form visible colonies in culture) are usually harmful [19-21].

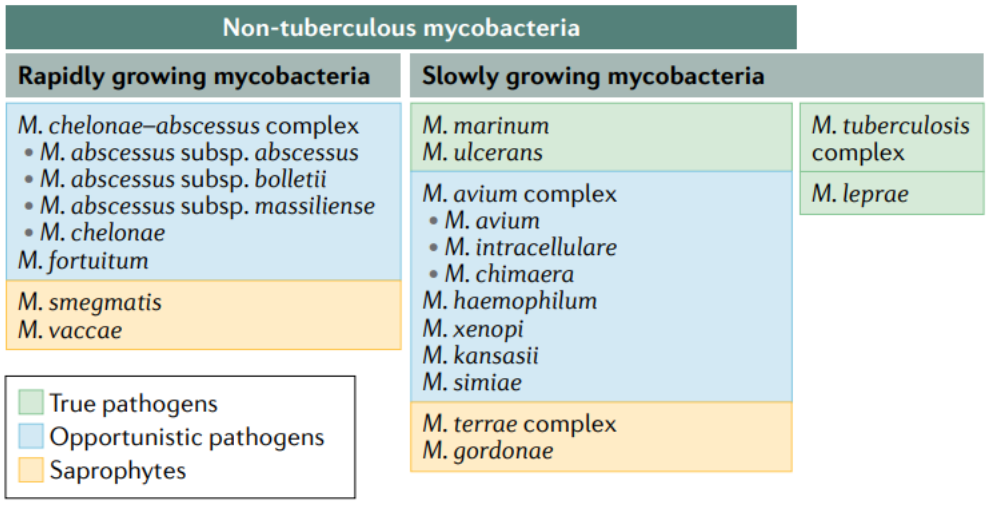

Figure 2 – Classification of the three major groups of mycobacteria: the *M. tuberculosis* complex, *M. leprae*, and non-tuberculous mycobacteria, regarding their rate of growth, as rapidly growing or slowly growing mycobacteria. The color distinction separates mycobacteria as being true pathogens, opportunistic pathogens, or saprophytes. Adapted from [19].

Tuberculosis (TB), caused by *Mycobacterium tuberculosis*, is a prominent cause of death among infectious illnesses that primarily affects the lungs in humans. In 2020, an estimated 9.9 million people fell ill with TB, and around 1.3 million people died from the disease [22]. The World Health Organization (WHO) has carried out several organized actions to end TB, included in the END TB Strategy [23], which aims to end the TB pandemic by 2035. Yet, with little success, TB infections are still quite prevalent. Of note, while the number of new TB cases has been slowly decreasing, the number of new NTM infections detected has been increasing, which may be due to better diagnostic tools [24].

1.1.1. Non-tuberculous mycobacteria

NTM, often known as "atypical mycobacteria", are a group of around 170 mycobacterial species that can cause pulmonary and non-pulmonary disease [24, 25]. Despite the improvement in diagnostic techniques [24], the incidence and prevalence of NTM infections are underestimated in most countries, because NTM-related infections are not mandatorily reported to public health authorities. Furthermore, NTM infections are often underappreciated in many TB-endemic countries, as both NTM and *M. tuberculosis* have the same reaction to the acid-fast staining method [24]. While the incidence of TB infections has remained stable over the past decade, the incidence of NTM infections has been rising, which emphasizes the epidemiological importance of NTM as human pathogens [26, 27]. According to a global survey carried out in 2008, approximately half of the NTM isolated obtained from human pulmonary species belonged to the *Mycobacterium avium* complex (MAC). This prevalence had some geographical variability, with MAC corresponding to 37% of European isolates, 52% of North American isolates, and 71% of Australian isolates [28]. In Portugal, an assessment of NTM cases reported between early 2002 and late 2012 identified an increasing incidence of NTM infections, in which MAC was the most frequently isolated [29]. In contrast to TB, pulmonary NTM infections are more common in women (59%) and the elderly (median age of 66 years-old) than in younger males, with MAC being the most common NTM species found in these infection cases [24]. Of note, because NTM infections do not respond to anti-TB medications, their therapy must be tailored to the type of infecting bacteria [24, 30, 31].

M. avium is an opportunistic intracellular pathogen that persists mostly within macrophages and evades the host's immune system [16, 30]. Glycopeptidolipids present in the cell wall may have an impact on this process [30]. Additionally, *M. avium*'s inherent and acquired resistance to antimicrobial treatment is related to mechanisms involving the degradation or extrusion of antimicrobials, the development of biofilms, or even mutations in genes that affect the mechanism of action of the drugs [30].

1.2. Mycobacterial infection

Mycobacterial infections may affect a variety of anatomical locations in the human host, like the bones or lymph nodes, but as they mainly invade mucosal and skin barriers, the most common clinical presentations are pulmonary or cutaneous infections [20]. The clinical range of illnesses caused by mycobacteria is widely determined by the host's susceptibility factors. Therefore, there are several diseases that increase the risk of mycobacterial infections, such as chronic obstructive pulmonary disease, cystic fibrosis, immunological insufficiency, and HIV, among others [24]. While *M. tuberculosis* is transmitted by direct contact with infected hosts, NTM transmission between humans is rare. The most common form of infection with NTM species is by direct contact with contaminated sources, particularly tapped water [32].

The mechanisms that control the course and outcome of mycobacterial infection are numerous, and they include a complex interplay between the host's immune system and the bacilli's survival tactics [33]. In the initial phases of the immune response, the phagocytosis of the invading mycobacteria occurs [34]. For example, inhalation of aerosols or airborne droplets containing *M. avium* leads to their spread through the lung's alveolar spaces. Following mycobacteria colonization of the lung, immune cells from the surrounding area such as macrophages (alveolar macrophages in this case), neutrophils, and monocytes, are drawn to the infection site and phagocytose mycobacteria [35]. Most NTM species are constrained by the innate immune response at this point.

Although macrophages are regarded to be an excellent first line of defense against bacterial infections, pathogenic mycobacteria like *M. avium* have evolved a variety of ways to survive within these cells. *M. avium* is capable of escaping elimination by macrophages through various mechanisms, such as the prevention of vacuole acidification, inhibition of

the influx of toxic products such as nitric oxide, or avoidance of autophagic and/or apoptotic killing [36-38]. These survival mechanisms modulate some phagosome's characteristics, allowing the organism to resist elimination and proliferate at a modest rate during the early phases of infection [38]. The progress of the infection would be largely determined by the host's immunological response later on. Upon mycobacterial infection of an immunocompromised host, an acute infection develops, characterized by uncontrolled bacillary multiplication, and the spread of the organism to distant areas. If the infected host is immunocompetent, the immune system will often resolve the initial infection, or hold it out *via* mechanisms that restrict additional bacillary multiplication, limit the spread of the organism, and target the immune response directly to the infection sites [33]. Bacteria are thought to be carried into deeper tissues, namely lymph nodes by macrophages and other phagocytic cells such as neutrophils after the phagosome's defense mechanisms are triggered, resulting in an early inflammatory response [19, 37]. Surprisingly, the macrophage serves as both the principal unit of cellular defense and the major location of bacterial proliferation and dissemination during the infection [31, 39].

In this early stage of infection, when macrophages are infected with *M. avium* for instance, an immune response begins and leads to the production of pro and anti-inflammatory cytokines [19, 39]. These infection-related signals drive the recruitment and influx of neighboring immune cells to the infection site, resulting in the creation of granulomas [19, 31]. Granulomas are histopathological entities that are characteristic of mycobacterial infection, and they reflect a dynamic host-pathogen interface that generally contains the infection [39, 40]. They surround spots of infected cells like macrophages, and are well-organized, dynamic collections of immune cells at varying stages of development, such as macrophages, monocytes, and neutrophils, among others [33, 39]. In addition to the presence and importance of immune innate cells, adaptive immunity also plays a key role in granuloma development and maintenance, as lymphocytic effector cells such as CD4+ and CD8+ T cells and B cells surround the granuloma's core [33]. Apart from physically sequestering mycobacteria, granulomas also suppress bacterial development by exposing them to stressors such as malnutrition, reactive oxygen species, and hypoxia [31, 33, 40]. However, the mycobacteria inside the hypoxic environment may persist in a dormant state and be reactivated afterward, leading to the onset of the active disease once again [39, 41].

Of note, TNFα and IFNγ are important mediators regarding the host's response to mycobacterial infections [42]. During mycobacterial infection, TNFα is mainly produced by macrophages [37], while IFNγ is secreted mostly by T cells [42]. It has been documented that TNFα levels exert an important role during the mycobacterial infection, as low levels or even the absence of this cytokine have been related to more susceptible and deathlier *M. avium* infections, due to poor phagocyte activation [43]. On the other hand, its excessive production leads to an exacerbated inflammatory response that hampers the clearance of bacteria and increases tissue damage [44]. TNFα is involved in the apoptosis of infected cells, while being essential to the formation of the granuloma structures [42-44]. These effects synergize with IFNγ, whose protective action against mycobacterial infections has been well-established [42]. IFNγ has the ability to contain the infection either by restricting the bacteria replication or by enhancing the phagosome and granuloma development [45]. Furthermore, the absence of IFNγ, either by antibody blockade or genetic deficiency, leads to an exacerbation of the mycobacterial disease [37, 46]. TNFα and IFNγ act in a concerted manner during *M. avium* infection. IFNγ instructs macrophages to enhance TNFα production [37], which will then activate the macrophages in an autocrine manner [47]. Then, both cytokines will exercise their antimycobacterial activity to fight the mycobacterial infection.

Chapter 2. The Bone Tissue

The skeleton allows the body's movement and locomotion, and its homeostasis is achieved by the constant remodeling of the bones. The bone is a tough, inflexible connective tissue [48, 49]. The strength and rigidity of the bones support the body, and they also act as an anchor site for muscles [48-50]. Moreover, bones protect vital organs such as the heart and the brain. The bone marrow, the major site of blood cells formation after birth, is found within the bone structure. The bones also serve as a storage site for growth factors and cytokines and maintain mineral homeostasis due to their calcium and phosphate reserves [49, 50]. The constant mechanical demands imposed on the body are counteracted by the high density and vascularity of the bones. Furthermore, the high cell density of the bones allows them to maintain an adequate bone mass and to eliminate potential micro-damage upon injury [48, 50].

2.1. Bone Structure

At the macroscopic level, the bone is white and has an heterogenous texture. Regarding their structure, bones are categorized as compact or trabecular (**Figure 3**). The proportions of compact and trabecular bone vary between and within the different bones. The compact bone is very dense and thick; it usually limits the outer layer of the bone, conferring strength and creating stiff articular surfaces [48, 51]. On the other hand, there is the trabecular bone, a porous, honeycombed type. While compact bones are mostly found in the diaphysis, the trabecular bones are found in the epiphysis, providing strength in compression. Additionally, during growth, compact and trabecular bones perform different roles, since the former is responsible for appositional growth and the latter is responsible for longitudinal growth [48, 51].

Depending on the age and location, the internal cavities of the trabecular bone are frequently filled with hematopoietic tissue and/or fat. Lining the interface between the bone marrow and the bone's internal surface is the endosteum which contains bone-forming cells and their progenitors. Lining the outer surface of the bone is the periosteum, which is also rich in bone-forming progenitor cells and usually responsible for the repair of fractures [51]. Additionally, Howship's lacunae are also present on the bone surface and represent a cavity of bone resorption where the bone-resorbing cells lay [48].

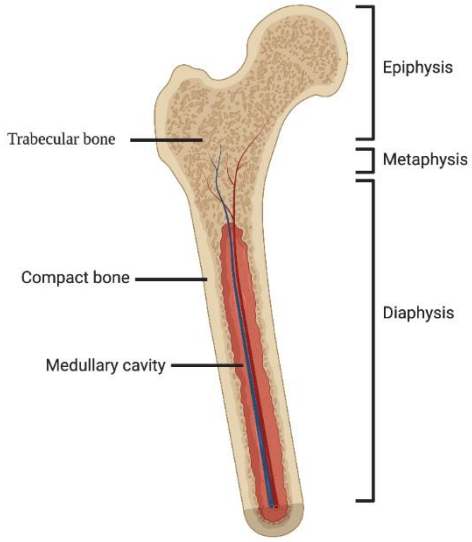

Figure 3 – Bone structure. Anatomical division and types of bone present in long bones. The compact bone is present in the external part of the bone, while the trabecular bone can be found deeper in the bone structure. Hematopoietic tissue and/or fat usually fill the internal cavities of the trabecular bone. Reproduced from [51].

At the microscopic and cellular level, the bone tissue consists of cells with specific functions that are within an extracellular matrix. Water makes up around 10 – 20% of bone mass, while the organic component makes up about 30 – 40% of the remaining dry weight. The percentage of organic components varies with age, location, and metabolic condition, and type I collagen fibers account for around 30% of the total organic matrix, playing an important role in bone cohesion and toughness. Inorganic mineral salts are present in the form of microcrystalline hydroxyapatite, which gives bone its hardness and a lot of stiffness. Mineralization rises with age, while bone mass declines [48].

The cellular components can be divided into two groups (**Figure 4**), the osteoblasts, which are the cells responsible for bone formation, and the osteoclasts, the cells capable of destroying the bone. Tight control and interaction between these cells are required to maintain an optimally balanced bone mass, and any change in the physiology of one cell type will dysregulate the activity of the other [51].

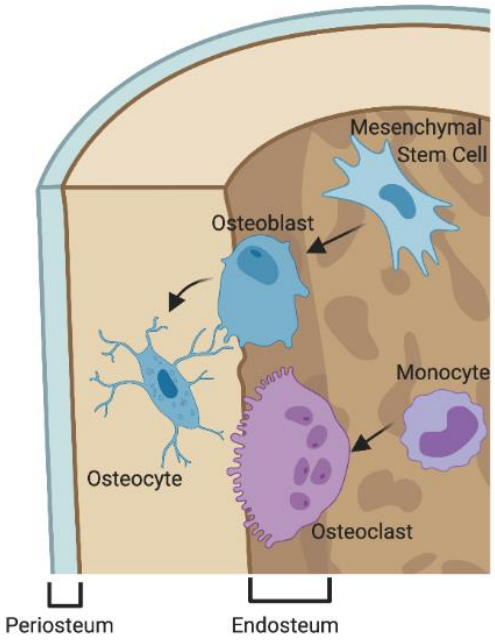

Figure 4 – Bone cellular components and their cellular precursors. Osteoblasts are derived from mesenchymal stem cells and form new bone by deposition of extracellular and mineral matrix. When osteoblasts become entrapped in the newly formed bone, they mature into osteocytes. In turn, osteoclasts, which are large multinucleated cells, have a myeloid origin and are responsible for bone degradation. Reproduced from [51].

2.1.1 Osteoblasts

Osteoblasts are bone-forming cells that layer the surfaces of developing or remodeling bone, residing in close contact with other bone cell types. Osteoblasts synthesize, secrete, and deposit the bone matrix that later becomes mineralized. These cells are derived from pluripotent mesenchymal stem cells (MSC) found in the bone marrow and other connective tissues [50-53]. Besides giving rise to osteoblasts, MSC are also capable of differentiating into adipocytes (fat cells), and chondrocytes (cartilage cells) [50-53]. RUNX2 and OSTERIX, two master transcription factors, are required for MSC to undergo osteoblastic development [53]. Deletion of either transcription factor results in the deficiency of osteoblasts *in vivo* [54]. These transcription factors regulate the expression of genes involved in the formation of the bone matrix, like the ones that express collagen type I alpha 1, and osteopontin [51, 53]. MSC differentiation is controlled by several pathways. The WNT pathway, is the most significant and well-described of them all. Moreover, the WNT

pathway has discovered to limit MSC differentiation towards adipocytes and/or chondrocytes, thus enhancing MSC to osteoblast differentiation [53, 55].

Osteoblasts secrete and generate components and proteins that are main constituents of the bone extracellular matrix, such as collagen fibers, osteocalcin, and osteonectin. Osteocalcin is a protein that binds hydroxyapatite and calcium and is important for bone mineralization and the growth of new bone. In addition to hydroxyapatite, osteonectin binds to collagen fibers [48, 51]. Moreover, osteoblasts produce the ligand for the receptor activator of nuclear factor kappa-B (RANKL). This ligand may bind to the receptor activator of nuclear factor kappa-B (RANK), present on the surface of osteoclasts and their progenitors, or to osteoprotegerin (OPG), a decoy receptor of RANKL that antagonizes its action. In order to make new bone, osteoblasts secrete osteocalcin and release alkaline phosphatase and pyrophosphatase, thus raising the local concentration of calcium and phosphate which leads to the beginning of mineral crystal formation. [48, 51, 53].

2.1.2. Osteocytes

Osteocytes are the most numerous bone cells, and they arise from osteoblasts that become entrapped in the mineral matrix. Osteocytes are joined by multiple dendritic processes to form a complex cellular network that regulates bone remodeling by releasing hormones and sensing mechanical loads in bone. Osteocyte death leads to matrix resorption by osteoclast activity [48, 53]. Functionally, osteocytes regulate both osteoclasts and osteoblasts. Regarding bone destruction, osteocytes secrete RANKL and OPG, thus enhancing or impairing osteoclast differentiation, respectively [56]. Concerning bone formation, osteocytes are a source of factors such as WNT1 proteins that enhance osteoblastogenesis [57], while also impairing osteoblastic development through the production of inhibitors of the WNT pathway such as DKK1 [56].

2.1.3. Osteoclasts

Osteoclasts are the only cells known to be capable of resorbing bone. They are large, multinucleated, and mitochondria-rich cells. Additionally, osteoclasts contain several vacuoles in their cytoplasm, including acid-phosphatase-positive lysosomes. Osteoclasts have hematopoietic origin and in the adult bone marrow, the conventional process of osteoclast formation involves the differentiation of HSC into a common myeloid progenitor

stage, which then differentiate into monocyte/macrophage lineage cells that must differentiate and mature before they can perform their full role [48, 50, 51, 53]. Upon differentiation from the common myeloid progenitors, macrophages origin osteoclast precursors (OCP) when stimulated with the macrophage colony-stimulating factor (M-CSF) and RANKL. OCP are found in bone marrow and circulation, and they are drawn to potential resorption sites in order to undergo fusion events that will origin osteoclasts. When RANKL binds to RANK on the surface of OCP, TRAFs (TNF-associated factors) signaling pathways will be activated, especially TRAF6. The formed RANK/TRAF6 complex will lead to the activation of signaling pathways including NF-kB, AP-1, and MAPK. Furthermore, these signaling cascades will initiate the expression of transcriptional factors such as NFATc1 and c-Fos, which will later promote the transcription of osteoclast-specific genes required for the resorbing activity of osteoclasts [58, 59]. Bone marrow stromal cells and osteoblasts are the major producers of M-CSF and RANKL, required for osteoclast differentiation [49-51]. However, M-CSF can also be produced by other cells such as monocytes [60] or chondrocytes [61]. Nevertheless, while it has been found that M-CSF is essential for the differentiation of osteoclasts [62], this process is not RANKL-dependent, as other factors such as TNFα are able to enhance osteoclast differentiation when RANKL is absent [63, 64].

Osteoclasts produce high levels of tartrate-resistant acid phosphatase (TRAP), cathepsin K (CatK), calcitonin receptor, and αvβ3-integrin. Therefore, these proteins are used as markers to detect osteoclasts *in situ* [51, 65]. Osteoclasts are responsible for the removal of bone in specific areas during bone development and remodeling. Signals from local cells (including osteoblasts, macrophages, and lymphocytes) and hormones like parathyroid hormone (PTH) induce osteoclasts to resorb bone. Their capacity to dissolve bone minerals is dependent on the secretion of hydrogen ions by v-ATPases, which creates locally an acidic environment, whilst they remove organic matrix by secreting lysosomal (CatK) and non-lysosomal (e.g., collagenase) enzymes [48, 50, 51, 66].

2.2. Modes of Osteoclast resorption

The “bone resorption cycle” assumes that osteoclasts must remain stationary during bone resorption but may move between intervals of resorption. The ability of osteoclasts to resorb the bone requires the coordination of the processes of mineral and collagen solubilization. Inhibitors that interfere with the rate of either collagenolysis or demineralization affect the resorptive activity of osteoclasts [67, 68]. When the rate of collagenolysis vs demineralization is reduced, the osteoclasts preferentially form circular, perpendicular excavations. These structures were regarded as intermittent resorption, or short-term resorption episodes interrupted by migratory phases. That is, the osteoclasts move along the bone surface performing punctual excavations [68, 69]. They correspond to the well-described “pit” mechanism (**Figure 5**) [70]. Osteoclasts become polarized in the process of bone erosion when they contact with activation signals. They erode bone when the ruffle border contacts with the bone surface. The ruffle border represents an area of the plasma membrane of osteoclasts that is surrounded by the sealing zone (SZ), which delimits the resorption compartment and marks the area of bone to be eroded [70]. On the other hand, increased collagenolysis versus demineralization rates result in a higher presence of extensive and deep resorption structures, known as “trenches” (**Figure 5**). They correspond to long-duration continuous resorption events in which the osteoclasts resorb bone while moving [67, 68]. It’s important to remember that pit development is merely the beginning of a much bigger resorption process for many osteoclasts (typically days in bone resorption assays) [70]. When compared to the pit resorption mode, the trench mode has better resorption performance in terms of time, speed, and depth, and is thus a marker of more aggressive bone resorption activity [67, 69, 70].

If excessive demineralization activity occurs, collagen will immediately function as a brake, avoiding the unnecessary resorption of the bone [70]. When collagen breakdown is as faster as demineralization, this brake is not engaged, and the SZ is able to move in the existing crater. Interestingly, collagen remnants are virtually always seen in pits, indicating that collagenolysis has been slower than demineralization, resulting in collagen buildup that stops the SZ from moving in the pit and preventing the transition to the trench mode. On the other hand, collagen remnants are not present in trenches, indicating that the collagenolysis has occurred at the same rate as demineralization, allowing the SZ to flow along the cavity’s

walls, enlarging them [68-70]. Osteoclasts abundantly express CatK, which in turn is the most powerful collagenolytic proteinase known among all mammalian proteinases, and, as a result, CatK-driven collagen breakdown is required for trench formation [67-70].

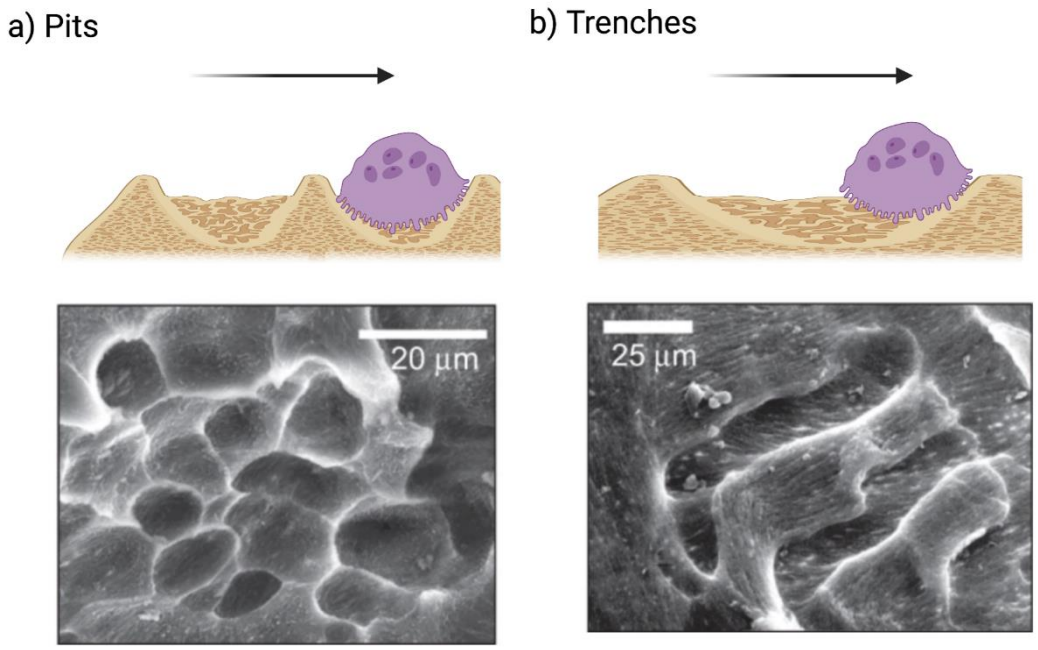

Figure 5 – Osteoclasts' resorption mechanisms. (a) In the pit mechanism (upper panel), osteoclasts perform intermittent resorption episodes in the bone surface, followed by migratory phases. The *in vivo* image obtained with scanning electron microscopy (SEM) (lower panel) shows an area with a resorptive pattern, resembling pits. **(b)** The trench forming mechanism (upper panel) is characterized by extensive, deep, and long-duration resorption episodes performed by osteoclasts, integrating resorption and migration in just one activity. The SEM image (lower panel) shows a clear area with signs of continuous resorptive activity, resembling trenches. Both the upper representative illustrations in **(a)** and **(b)** were created using BioRender.com. The lower SEM images in **(a)** and **(b)** were obtained from [68] under the terms of a CC BY 4.0 license: https://creativecommons.org/licenses/by/4.0/ (accessed on 15 February 2022).

Usually, bone resorption assays are performed *in vitro*, using bone slices to simulate the resorption activity of osteoclasts. The detection of this activity *in vivo* can be performed through SEM techniques, for example. The resulting images from this method, which are commonly utilized to detect extensive erosion in osteoporotic patients' bone surfaces, revealed a significant incidence of trenches [68, 70]. This observation indicates that trenches are formed not only in resorption assays, but *in vivo* as well, and their presence appears to be largely underestimated. Altogether, it seems that the trench mechanism has a role in

pathological bone resorption [70]. Given this, the resorption activity of osteoclasts should not only be assessed by the extension of bone erosion, but also by distinguishing the resorption resulting from osteoclasts showing a pit or trench behavior [69].

2.3. Bone remodeling

Bone remodeling refers to the concerted action of osteoclast bone degradation and osteoblast bone rebuilding to ensure mineral equilibrium [50, 71]. Alterations in the mineral equilibrium are used to define the advance of certain bone diseases, like osteoporosis [50, 71]. Through remodeling, old bone zones are removed and replaced with new ones containing freshly proteinaceous matrix, which will be mineralized to complete the new bone formation. Even before birth, the process of bone remodeling already occurs, and it continues throughout life [50].

The tightly connected action of osteoclasts and osteoblasts is sequentially performed in order to repair bone damage, thus preventing the formation of new bone over damaged bone [50]. The activation phase, resorption phase, reversal phase, formation phase, and termination phase are the five steps of bone remodeling [53]. Emerging evidence supports the hypothesis that bone remodeling takes place within a closed, high vascular system called the bone-remodeling compartment (BRC), covered by bone-lining cells [49]. Therefore, the bone remodeling process (**Figure 6**) follows these stages [49, 50, 53, 71]:

(1) Activation phase in which local mechanical or hormonal impulses begin bone remodeling. Osteocytes are thought to sense and transduce these signals into a biological response in the bone, where local regulators like M-CSF and RANKL, and systemic regulators such as PTH, estrogen, calcitriol, and calcium, will promote osteoclastogenesis, and drive osteoclast precursors to undergo differentiation within the BRC.

(2) During the resorption phase, mature osteoclasts release protons and proteases, like CatK and matrix metalloproteinases (MMPs), to degrade both mineral and organic matrix.

(3) The reversal phase consists of the death of mature osteoclasts, which is promoted by the expression of the FAS ligand following estrogen induction. Also, osteoblasts are guided to the resorption site by local molecules such as transforming growth factor beta and start bone formation.

(4) The formation phase lasts around 4 to 6 months, during which osteoblasts take over the bone rebuilding process. Osteoblastogenesis will be induced by regulators like WNT and PTH. The osteoid (new bone matrix), which is made up of various proteins such as type I collagen, begins to deposit until the whole compensation for bone resorption has been accomplished. To maintain a balance between bone loss and bone growth, osteoblast function will continue even after the cessation of bone resorption.

(5) During the termination phase, osteoblasts either undergo apoptosis or generate new osteocytes. As hydroxyapatite is deposited, bone mineralization will begin and finish during this period.

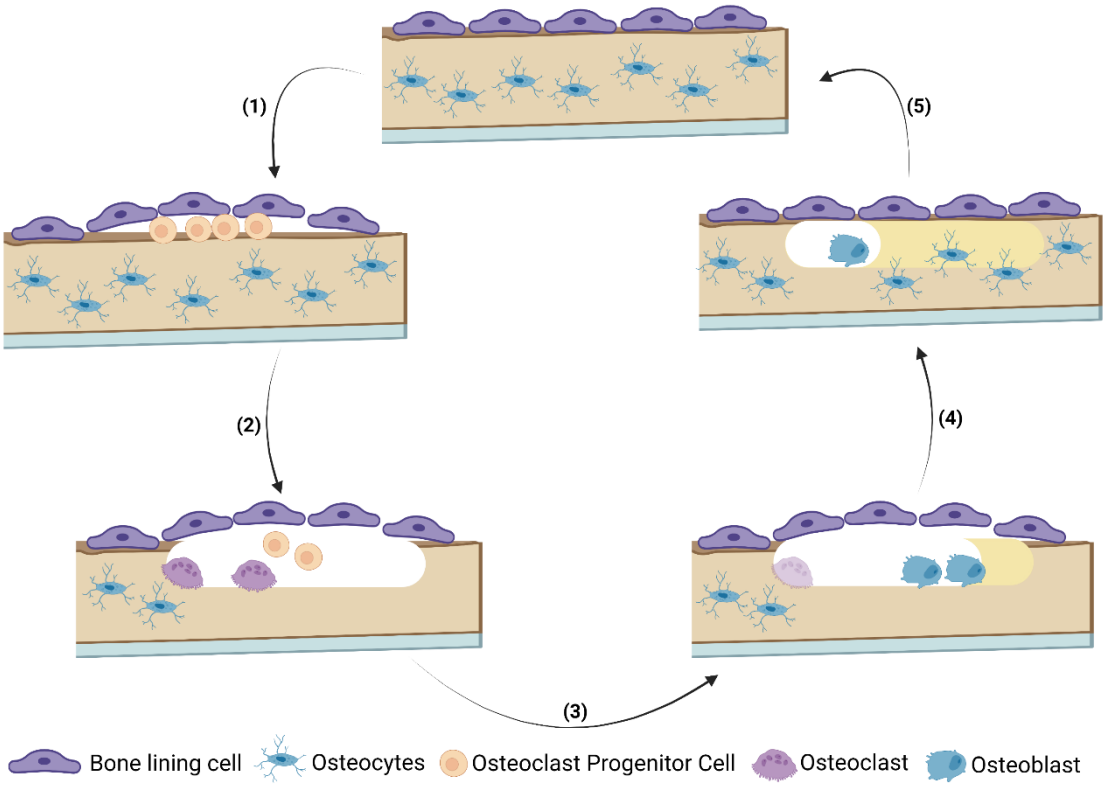

Figure 6 – Representation of the bone remodeling process. Local hormonal or mechanical impulses are sensed by osteocytes and drive osteoclastogenesis to occur within the bone-remodeling compartment (BRC). Mature osteoclasts degrade both mineral and organic matrix (white area), and osteoblasts are recruited to the resorption site. Osteoblasts take over the bone remodeling process and begin the formation of the osteoid (gold color area) while osteoclasts undergo apoptosis. Finally, when the growth of the new bone is completed, osteoblasts either undergo apoptosis or generate new osteocytes. Figure was created using BioRender.com.

2.4. Crosstalk between bone cells

As described above, the process of bone remodeling requires a tight crosstalk between osteoclasts, osteoblasts, and osteocytes, which is summarized in **Figure 7**. Osteoblasts regulate osteoclasts through the production of M-CSF and RANKL. These factors will bind to their receptors on the surface of OCP and osteoclasts, thus promoting their survival, differentiation, and further resorptive activity. Additionally, osteoblasts avoid excessive osteoclast proliferation by the secretion of OPG, which will then act as a decoy receptor sequestering RANKL [51, 66]. Furthermore, osteoblasts secrete proteins such as WNT5A or WNT16, which promote or inhibit osteoclast differentiation, respectively [58, 66]. On the other hand, osteoclasts also control osteoblast development through the secretion of soluble factors that can either enhance osteoblastogenesis, such as S1P or suppress it, like SEMA4D [66]. Moreover, osteocytes also contribute to the crosstalk between the bone cells, modulating osteoclastogenesis by the production of RANKL and OPG, and controlling osteoblastogenesis while producing WNT1 and DKK1 proteins [51, 53].

Osteoclast and osteoblast activities are also highly regulated by several hormones and vitamins, in order to secure a balanced bone mass. PTH is one of the endocrine factors that help regulate bone homeostasis either by enhancing bone degradation or bone formation [72]. It is secreted after sensing low serum calcium levels and its continuous production increases bone resorption, by enhancing RANKL production and decreasing OPG secretion by osteoblasts. As bone resorption increases, more calcium is released [72, 73]. Additionally, it has been documented that intermittent PTH secretion leads to an anabolic action of this hormone, as PTH directly induces WNT signaling and RUNX2 expression, increasing bone formation by osteoblasts [72, 73]. Amongst other endocrine factors, estrogen also plays an important role in the control of bone homeostasis. It has been found that estrogen induces the expression of Fas ligand in osteoclasts, leading to their apoptosis, which leads to decreased bone resorption [74]. Additionally, others have documented that estrogen deficiency in women due to menopause or ovariectomy leads to high bone turnover, correlating with decreased bone mass [75]. Finally, Vitamin D may also influence bone metabolism, as it stimulates the differentiation of MSC towards the osteoblast lineage [50, 51].

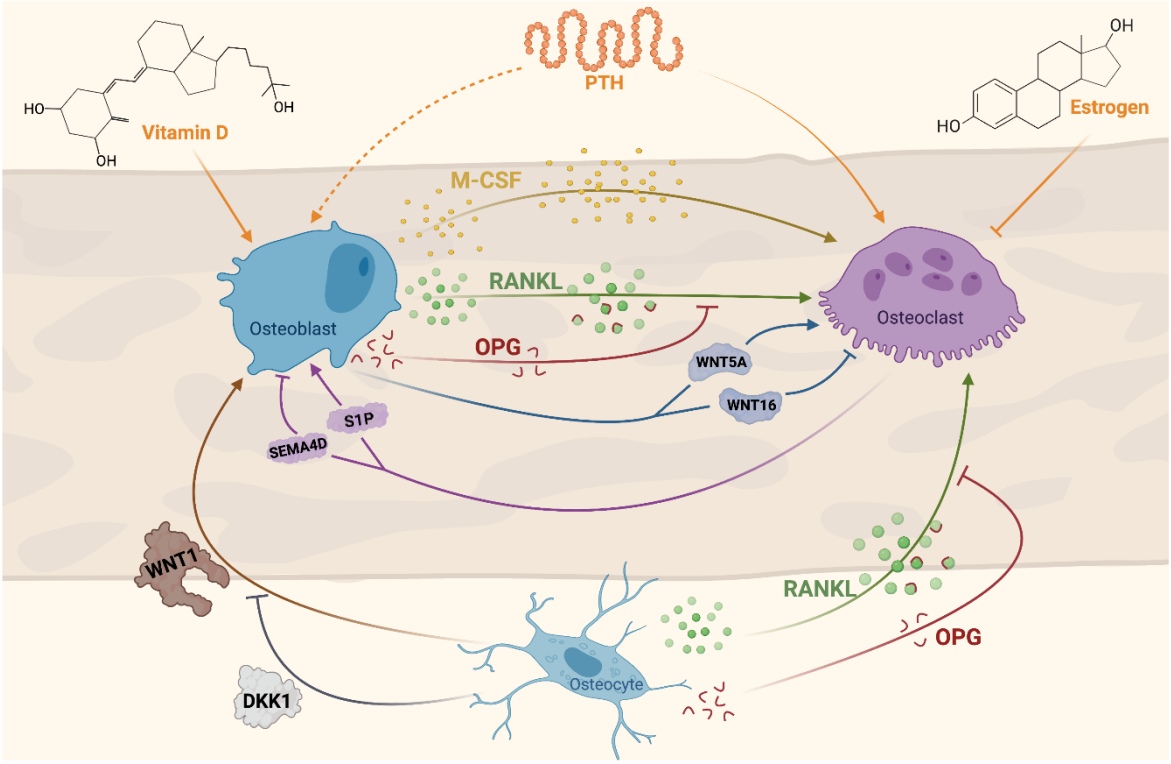

Figure 7 – Crosstalk between the bone cells. Osteoblasts modulate osteoclastogenesis, enhancing it by the production of M-CSF, RANKL, and WNT5A, and repressing it through secretion of OPG and WNT16. On the other hand, osteoclasts also control osteoblast's development, by secreting proteins such as S1P and SEMA4D. Osteocytes modulate both osteoclastic and osteoblastic differentiation. Furthermore, hormones and vitamins also regulate bone cells development. While estrogen impairs osteoclastogenesis, vitamin D enhances osteoblastogenesis. Moreover, continuous PTH secretion augments the development of osteoclasts, while its intermittent secretion favors osteoblastic differentiation. Figure was created using BioRender.com.

2.5. Inflammatory bone loss

Bone health is critically important to the overall wellbeing and quality of life in humans. Disruption in bone mass homeostasis will lead to either increased or decreased bone mass. Bone loss-associated pathologies arise when osteoblastic activity is diminished and/or there is excessive bone resorption, as it is observed in osteopenia [76]. In more severe cases, osteopenia will advance to osteoporosis [53]. The microdamage suffered by the bone will be translated into bone fragility, causing osteoporosis-related fractures. Fragility fractures, or low-impact fractures, arise after intrinsic alterations in the bone structure, namely the imbalance of bone remodeling, which will cause the break of the bone when it is subject to mechanical stresses that, normally, wouldn't lead to a fracture [53, 77]. Fragility fractures decrease quality of life due to prolonged immobilization and clinical deterioration of

preexisting diseases. Moreover, low-impact fractures also pose economical strains for patients and health systems. Hence, the earliest identification and therapeutic intervention of those individuals with low-bone mass is fundamental to prevent this snowball.

Osteomyelitis is a difficult-to-treat bone infection caused by an invading microbe colonizing one or more bone compartments and is also associated with bone loss [78]. The bone colonization by pathogens triggers a local inflammatory response, which leads to bone lysis over time. These infections tend to occur because of the spread of pathogens already present in the host, or when a region, which suffered trauma, contacts with a contaminated source [78, 79]. *Staphylococcus aureus* is by far the most usually implicated bacterial pathogen in osteomyelitis [80]. Mycobacteria are also capable of infecting the bone. Examples of these organisms are *M. tuberculosis* [81], and *M. avium* [82]. Despite surgical and chemotherapeutic advances, there is no commonly acknowledged plan to treat osteomyelitis, as infection occurs in an avascular environment, where antibiotics are not capable of penetrating [83].

Of note, low bone mass may also arise as a consequence of chronic inflammatory diseases, such as rheumatoid arthritis, inflammatory bowel disease, or even chronic obstructive pulmonary disease, among others [84]. In these inflammatory conditions, immune mediators such as pro-inflammatory cytokines are produced and, among other actions, stimulate osteoclastic bone resorption, which leads to bone loss [85].

2.5.1. Known players produced during infections that cause bone loss

Increased production of inflammatory factors, due to infections e.g., has been correlated with bone loss [84, 86]. Here, the mediators previously implied in bone loss as a collateral damage during mycobacterial infection will be addressed.

2.5.1.1. TNFα

TNFα is a pro-inflammatory cytokine that is mostly produced by macrophages and activated T cells [51], and has a role in the enhancement of autophagy [86]. Autophagy is a normal cell process that regulates the degradation of intracellular components, namely intracellular pathogens, which helps the cell avoid apoptosis, and, when dysregulated, also leads to bone abnormalities [86, 87]. In the context of the bone, TNFα production is induced

following bone trauma, like fracture [88] or bone infection [84]. It has been demonstrated that TNFα can inhibit the apoptosis of osteoclasts infected with mycobacteria, as it activates autophagy mechanisms to eliminate the invading pathogen [86]. Furthermore, TNFα is known to increase the proliferation of osteoclast precursors *via* the RANKL pathway, thus leading to the development of osteoclasts and, consequently, to higher resorptive activity [89, 90]. That said, TNFα not only has an important role in controlling the cell fate during infection but also contributes to increased osteoclast activity. [90]. TNFα has dual effects on osteoblastogenesis, as it either encourages MSC differentiation towards the osteoblastic lineage [91] or represses osteoblastic development [92], also inducing osteoblast apoptosis [93].

2.5.1.2. IFNγ

IFNγ has an active role in antiviral and antibacterial immunity, enhancing macrophage activation, for example [94]. However, regarding bone homeostasis, the role of this cytokine is controversial. IFNγ is well defined to promote osteoblastogenesis. By inhibiting adipogenic differentiation, through upregulation of the transcription factor RUNX2, IFNγ stimulates MSC differentiation into osteoblasts [94]. On the other hand, IFNγ secreted by immune cells like B, Natural Killer, or T cells directly inhibits osteoclastogenesis, by increasing the degradation of TRAF6 or downregulating NFATc1, for instance. Moreover, this cytokine also promotes osteoclast apoptosis by inducing FasL expression, thus, its action can be characterized as directly anti-osteoclastogenic. In contrast, IFNγ is also known to influence cells like macrophages to secret the C-X-C motif chemokine ligand 10 protein, which, in turn, stimulates T cells to produce RANKL and TNFα that will favor the differentiation of osteoclasts. Thus, IFNγ is also pro-osteoclastogenic in an indirect way and has dual roles concerning bone resorption [51, 94, 95].

2.5.1.3. SAA3

Although not commonly associated with bone homeostasis as the previous cytokines, the acute-phase protein SAA3 [96] also has an important function in bone loss.

The family of SAA proteins comprehends four genes, namely *Saa1*, *Saa2*, *Saa3,* and *Saa4* [97]. In humans, SAA1 and SAA2 are induced by the acute-phase response while SAA4 is constitutively expressed. In humans, the *Saa3* gene is described as a pseudo-gene.

On the other hand, mice express *Saa1*, *Saa2*, and *Saa3* [98]. Of note, although *Saa3* is a pseudo-gene in humans, phylogenetic studies have reported that the murine *Saa3* gene and the human *Saa1* gene have evolved into functionally analogous genes, also exhibiting high protein sequence homology, thus indicating a possibility for SAA3 to perform the biological functions of human SAA1 and SAA2 [96]. The SAA proteins were firstly correlated with amyloidosis events, acting as a precursor of amyloid deposits. They are proteins with low solubility in an aqueous medium, and, in blood, they can be found associated with high-density lipoproteins, thereby functioning as apolipoproteins [97-99]. SAA is highly expressed in the liver; however, this protein has been found in other cell types and tissues like monocytes/macrophages, adipocytes, or chondrocytes [96, 98-100]. Moreover, it has been described that *M. tuberculosis*-infected macrophages express *Saa*3, emphasizing the correlation between mycobacterial infections and the production of SAA proteins [101].

Regarding the bone tissue, SAA3 has been recently implicated in bone homeostasis. It has been found that SAA3 is produced by preosteoclasts, osteoblasts, and, even more, by osteocytes. This acute-phase protein is also capable of inhibiting osteoblast differentiation, through suppression of osteoblast-related genes, and enhance osteoclastogenesis, showed by the formation of multinucleated TRAP-positive cells [96, 99, 100]. Furthermore, SAA3 is sensed by MSC through Formyl Peptide Receptor 2 and Purinergic Receptor P2X 7 (P2RX7) [96, 100, 102], or by osteoclast precursors, osteoclasts, osteoblasts, and osteocytes as well through the P2RX7 receptor [96, 102]. SAA3 also modulates the expression of genes involved in bone matrix remodeling (*MMP13*), bone turnover (*C-C Motif Chemokine Ligand 5*), and apoptosis (*Fas*) [99].

Moreover, SAA3 has been associated with bone loss as a mediator of the PTH action. As mentioned above, continuous PTH secretion exerts a catabolic effect in bone turnover, enhancing bone resorption and impairing bone formation [72, 73]. PTH induces COX2, which in turn increases PGE_2 production, far leading to decreased bone formation [100]. Nevertheless, PGE_2 does not directly inhibits osteoblastic differentiation [103]. Instead, it has been documented that in the absence of the SAA3 protein, continuously administrated PTH has an anabolic effect in bone turnover. Thus, SAA3 induces the inhibitory action of the COX2/PGE_2 axis in the anabolic effect of continuous PTH, further leading to decreased bone formation [104]. This relation emphasizes the role of SAA3 protein in bone homeostasis, as it overrules the anabolic action of the PTH.

Altogether, SAA3 appears to be a protein that acts as a local regulator of bone turnover, reporting microdamage and having several functions associated with bone remodeling, bone resorption, and skeletal development [96, 99, 100].

Furthermore, increased levels of SAA have been associated with some chronic inflammatory diseases, such as rheumatoid arthritis, cardiovascular diseases, or Alzheimer's disease [96, 99]. In rheumatoid arthritis, SAA proteins have been used as a biomarker and have also been correlated with cardiovascular disease in these patients. Regarding cardiovascular diseases, SAA is believed to be implicated in the pathogenesis of atherosclerosis [97]. Additionally, SAA production seems to be enhanced by glucocorticoids, despite their capacity to reduce inflammation [105]. SAA has been recently involved in COVID-19, as a recent study has described that the systemic SAA levels are elevated in these patients [106, 107].

AIMS

Mycobacterial infections are often associated with comorbidities such as anemia, and a higher risk of osteoporosis [108, 109]. Previous studies from our research team have shown that in the murine model of *M. avium* disseminated infection, bone mass and mineral density are decreased in an IFNγ- and TNFα-dependent manner. Bone marrow parenchyma is colonized by mycobacteria but the bone tissue itself is not. Instead, mycobacteria reside mostly in macrophages within the bone marrow parenchyma [110]. Further studies highlighted that infection-driven bone loss is due to a dysregulation of bone turnover, with increased bone degradation and decreased bone formation. Additionally, targeted transcriptome analysis of whole bones indicated that the mostly differentially expressed gene in the bone during *M. avium* infection was *Saa3* which codes for the SAA3 protein (data not published). These observations led us to hypothesize that the production of IFNγ and TNFα in response to the ongoing mycobacterial infection drives the production of SAA3 that, in turn, disrupts bone turnover. In order to dissect the role of SAA3 in bone loss during *M. avium* infection, we defined the following specific aims:

1) Evaluate whether soluble molecules produced by infected macrophages enhance osteoclast formation and/or activity, leading to increased bone resorption during infection. Previous data from our lab have shown that *M. avium*-infected macrophages produce soluble factors that induce the formation of osteoclasts with an increased number of nuclei. In aim 1, we will further investigate whether the increased number of nuclei per osteoclast correlates with increased bone resorption activity, using pit assays.

2) Determine the cellular sources of SAA3 in the bone. As macrophages are the principal host of *M. avium* within the bone marrow parenchyma, we hypothesize that SAA3 is one of the soluble factors produced by infected macrophages that enhance osteoclastogenesis. Here, the expression of SAA3 by infected macrophages and other cells will be studied at the gene expression and protein levels.

3) Identify the role of soluble molecules produced by infected macrophages in osteoblastogenesis. Based on our previous data, it is likely that SAA3 is one of the soluble factors produced by infected macrophages, impairing the formation of new bone. In the last aim, we will determine how osteoblast formation is affected by SAA3 and conditioned media from *M. avium*-infected macrophages.

MATERIALS AND METHODS

Bacteria

The *inoculum* of *Mycobacterium avium* strain 25291 smooth transparent (SmT) variant was prepared and aliquoted as described in [110]. Aliquots were stored at -80 ºC until needed. Just before use, an aliquot was thawed and diluted to the desired concentration.

Mice

C57BL/6 and *Tnfalpha*$^{-/-}$ mice were bred and housed under specific pathogen-free conditions at the Instituto de Investigação e Inovação em Saúde (i3S) animal facility. Mice were housed at 22 ºC with a 12 h light/dark cycle in individually ventilated cages with HEPA filters and fed with sterilized food and water *ad libitum*.

Ethics statement and participants

All experimental and animal procedures described in this work were approved by the local animal ethics committee of the Instituto de Biologia Molecular e Celular/i3S and licensed by the Portuguese Authority General Directory of Agriculture and Veterinary (DGAV) on July 6th, 2016 (reference no. 00421/000/0002016). All animals were handled in strict accordance with good animal practice as defined by national authorities General Directory of Agriculture and Veterinary (Decreto-Lei 113/2013, August 7th) and European Directive (2010/63/EU).

Cytokines

M-CSF and RANKL were purchased from BioLegend (USA). Aliquots at 100 µg/mL were prepared by diluting the stock solutions in phosphate-buffered saline (PBS)1x / 1% bovine serum albumin (BSA) (Fisher Scientific, USA) and stored at -20 ºC until needed. TNFα was purchased from BioLegend, USA at a concentration of 200 µg/mL. Aliquots at 50 µg/mL were prepared by diluting the stock solution in PBS1x / 1%BSA and stored at -20 ºC until needed. IFNγ was purchased from PreproTech, USA and a stock solution of 200 µg/mL was prepared and stored at -20 ºC. Before using, a 200 ng/mL working solution was prepared. Recombinant Human Apo-SAA was purchased from PeproTech, UK, and 100 µg/mL aliquots were prepared by reconstitution in dH_2O/0,1% BSA.

Bone Marrow-Derived Macrophages

C57BL/6 mice were sacrificed, and the bones of the back hind were collected. Bone marrow was flushed with Dulbecco's Modified Eagle's Medium (DMEM, Gibco, UK), supplemented with 10% fetal bovine serum (FBS) (Invitrogen, USA), 1% HEPES, 1% pyruvate, and 1% L-glutamine (all from Gibco, UK), and cells were centrifugated at 1500 rpm for 5 minutes at 4 ºC. After centrifugation, cells were resuspended in DMEM with 10% L929 cell-conditioned medium (LCCM), plated in Nunc ™ EasYDish ™ Dishes (Thermo Fisher Scientific, USA), and incubated overnight in a humidified 37 ºC/5% CO_2 incubator. Non-adherent cells were collected by washing the plate with cold Hank's Balanced Salt Solution (HBSS, Gibco, UK), and centrifugated at 1500 rpm for 5 minutes at 4 ºC. Cell density was adjusted to 4×10^5 cells/mL in DMEM/10% LCCM. Cells were seeded in 6 well Tissue Culture Standard Flat Base plates (Sarstedt, Germany), and incubated in a humidified 37 ºC/5% CO_2 incubator. At day 4 of culture, 10% of LCCM was added to each well, and at day 7 of culture, the medium was renewed. At day 10, the supernatants were collected, filtered and aliquots were prepared, labeled, and stored at -80 ºC until needed. Then, *M. avium inoculum* was prepared with a cellular density of 5×10^6 cells/mL, and 800 µL were added to each well to infect the macrophages. After 4 h, the infection was stopped by washing the wells with warm HBSS for 3 times. Finally, cells were incubated with DMEM/10% LCCM, in a humidified 37 ºC/5% CO_2 incubator. During the 3 days post-infection, TNFα and IFNγ were added to the respective wells to achieve a concentration of 10 ng/mL and 16 ng/mL, respectively. DMEM was added to non-treated wells. At days 3 and 5 post-infection, the supernatants were collected, filtered and aliquots were prepared, labeled, and stored at -80 ºC until needed.

RNA extraction and Quantitative Real-Time PCR

Total RNA was extracted from BMDM and from bones of *Tnfalpha*$^{-/-}$ mice. **BMDM:** cells were lysed, and RNA was isolated according to the manufacturer's instructions in the PureLink RNA Mini Kit (Invitrogen). ***Tnfalpha*$^{-/-}$ bones:** previously frozen *Tnfalpha*$^{-/-}$ mice femurs were crushed in a liquid nitrogen bath and total RNA was isolated using PureLink RNA Mini Kit (Invitrogen). After RNA extraction and quantification, cDNA was synthesized using NZY First-Strand cDNA synthesis kit (NZYTech, Portugal) for further use in the quantitative real-time PCR reaction. *Saa3* expression was determined using *Gapdh*

as housekeeping gene in a CFX96 Touch Real-Time PCR Detection System (BioRad, USA). Then, qPCR data were analyzed using BioRad CFX Manager™ Software.

Primers sequences:
Gapdh Fw: 5'- TGTGTCCGTCGTGGATCTGA – 3';
Gapdh Rv: 5'- CCTGCTTCACCACCTTCTTGA – 3';
Saa3 Fw: 5' – ACATGTGGCGAGCCTACTCT – 3';
Saa3 Rv: 5' – GAGTCCTCTGCTCCATGTCC – 3'.

Osteoclast differentiation *in vitro*

Bone marrow was harvested from the bones of the back hind of C57BL/6 mice after flushing with complete αMEM (αMEM supplemented with 10% of fetal bovine serum and 1% of PenStrep (Gibco, UK)). Then, after the addition of RBC lysis buffer (NH_4Cl, $KHCO_3$, and EDTA) cells were centrifugated at 1500 rpm for 5 minutes and plated in Nunc™ EasYDish™ Dishes (Thermo Fisher Scientific, USA) overnight in complete αMEM supplemented with 10 ng/mL M-CSF, at 37 ºC/5% CO_2. Non-adherent cells were collected after plate wash with αMEM three times. Then, after centrifugation at 1500 rpm for 5 minutes, cells were counted, resuspended in OC media (αMEM / 100 ng/mL M-CSF / 100 ng/mL RANKL), and cultured at a cellular density of 7.5×10^5 cells/mL on the top of bone slices (boneslices.com, Denmark) in 96-well Flat Bottom Thermo Scientific™ Nunclon™ Delta Surface plates. This was considered the day 0 of culture. For morphological studies, 4titude® VisionPlate™ 96 well microplates (Black, clear base) were used. To study the effects of soluble factors produced by infected macrophages, the cultures were supplemented with 50% of supernatants from infected (INF) or non-infected (NI) BMDM cultures, maintaining a final concentration of 100 ng/mL of RANKL and M-CSF. To understand the impact of TNFα in osteoclast cultures, cultures were supplemented with 25 ng/mL of TNFα since day 0. To assess the effect of IFNγ, cultures were supplemented, since the beginning of the culture, with 1 ng/mL of IFNγ. The impact of M-CSF was studied in cultures performed as described before, but the concentration of this factor was altered to 150 ng/mL. To study the effect of the SAA protein, osteoclast cultures were supplemented with 5 µg/mL of Recombinant Human Apo-SAA (PeproTech, UK). Cells were then incubated in a humidified 37 ºC/5% CO_2 incubator. Media and cytokines were renewed every other day

and supernatants were collected, aliquoted, and labeled accordingly to the content of the well and the timepoint of culture.

Osteoclast immunofluorescence

At the 7th day of the osteoclast culture, cells were fixed with 4% paraformaldehyde (PFA) (BioOptica, Italy) for 10 minutes at room temperature (RT). Cells were washed 3 times with PBS1x and permeabilized with 0,1% Triton^{TM}X-100 / PBS1x / 2% FBS for 15 minutes at RT, and after this, were washed again with PBS1x. Cells were stained with DAPI (cat. no. D9564, Sigma Aldrich, USA) at 1:500 dilution, and with HCS CellMask^{TM} (cat. no. H32714, Invitrogen, USA) at 1:5000 dilution, for 1 h, RT and protected from the light. Lastly, cells were washed 3 times with PBS1x and kept in PBS1x at 4 ºC, protected from the light, until imaging. The cultures were imaged in IN Cell Analyzer 2000 microscope (GE Healthcare, USA), using 20x objective lens. The excitation and emission filters used to detect DAPI and HCS CellMask^{TM} were DAPI and FITC, respectively. This setup allows to identify the cell nuclei (DAPI) and the cell cytoplasm (CellMask^{TM}). Images were processed using the software IN Cell Navigator (GE Healthcare, USA) and ImageJ (National Institutes of Health, USA).

Osteoclast quantification

The quantification of multinucleated osteoclasts was manually performed using ImageJ and Microsoft Excel (Microsoft Corporation, USA). A multinucleated cell with 3 or more nuclei was considered an osteoclast, and the cells were divided in 4 categories according to the number of nuclei per cell: 3 to 4 nuclei; 5 to 10 nuclei; 11 to 20 nuclei and more than 20 nuclei. After counting, the results were represented in terms of the frequency of each category within each condition tested.

Quantification of osteoclast bone resorption activity

The resorptive activity of osteoclasts was determined through pit assays, in which osteoclasts were seeded on top of commercially available bovine cortical bone slices (boneslices.com, Denmark) previously submerged in αMEM for at least 1 h. Osteoclast cultures were performed as described above. At day 7 of culture, media was removed, and cells were incubated with water for 24 h at 4 ºC. Then, bone slices were washed in water and stained with toluidine blue (Sigma-Aldrich). The total numbers of resorptive events present

throughout the bone surface were counted using a 100-point graticule as a frame (using a total of 28-29 graticules per bone slice), fitted into the ocular of an Olympus BH2 optical microscope. The resorptive events were categorized as pits, represented by circular, perpendicular excavations, or trenches, which are extensive and deep resorption structures. The number of trenches per bone slice was compared to the number of pits. Samples were blinded before quantification of resorptive events.

Quantification of TRAP activity

The activity of TRAP was determined in the supernatants recovered from the osteoclast cultures, at different timepoints. The method used measures TRAP enzyme activity by the conversion/dephosphorylation of p-nitrophenylphosphate (pNPP) to p-nitrophenol (a yellow compound) in the presence of sodium tartrate (protocol adapted from [111]). Briefly, 10 µL of the supernatant sample were mixed with 90 µL of the previously prepared TRAP solution buffer (containing 12,5% L-Ascorbic acid (8,8 mg/mL); 12,5% DiSodium tartrate (46 mg/mL); 12,5% 4-nitrophenylphosphate (18 mg/mL); 25% Reaction buffer (1 M Acetate; 0,5% Triton X-100; 1 M NaCl; 10 mM EDTA ph=5,5) and 37,5% MilliQ water) in 96-well plates. The plates were incubated, protected from the light, in a humidified atmosphere at 37 ºC for 1 h. 100 µL of stop buffer (0,3 N NaOH) was then added to each well to stop the enzymatic reaction. The absorbance was read at 405 nm. Simultaneously, the total protein content of the samples was measured, using the Bio-Rad DC Protein Assay (Bio-Rad Laboratories, USA). A BSA standard curve was used and the absorbance at 655 nm was measured. TRAP activity was calculated using Microsoft Excel (Microsoft Corporation, USA) and expressed in nmol/min/µg of protein.

Osteoblast differentiation *in vitro*

Mice were sacrificed and hind legs were collected for isolation and expansion of mesenchymal stromal cells. After bone marrow flushing with complete αMEM, cells were resuspended in complete αMEM and seeded in Falcon® 25 cm² Rectangular Canted Neck Cell Culture Flask with Vented Cap (Falcon®, Corning, USA). Cells were incubated in a humidified incubator at 37 ºC, and 24 h later, non-adherent cells were removed and warm complete αMEM was added. Media was also changed every 2 to 3 days. At day 7 of culture, adherent cells were harvested after incubation with trypsin. Cells were counted in a Neubauer chamber, using Trypan Blue. Cell density was adjusted to 5×10^5 cells/mL, and 2

x 10^5 cells were seeded per well in 24-well Tissue Culture Standard Flat Base plates (Sarstedt, Germany). After 3 days, OB medium (20% MesenCult™ Osteogenic Stimulatory Supplement (OSS), 80% MesenCult™ MSC Basal Medium and 2 mM of L-Glutamine) was added. To study the effects of soluble factors produced by infected macrophages, the cultures were supplemented with 50% of supernatants from INF or NI BMDM cultures. In these studies, the plated cell suspension had the double concentration of OSS. To assess the effect of the SAA protein, the cultures were supplemented with 5 µg/mL of Recombinant Human Apo-SAA. Cells were incubated at 37 ºC and the medium was changed every 3 days until bone matrix formation was observed. Bone matrix formation took approximately 12 to 14 days.

Alizarin Red Quantification

At the (21st day) end of the osteoblast differentiation assay, cells were fixed with 4% PFA and washed 3 times with PBS1x. Then, alizarin red solution (Sigma) was used to stain the calcium deposits in the cultures, for 30 minutes at RT with gentle agitation. After this, wells were extensively washed with dH_20. The wells were photographed using an Olympus SZX10 stereomicroscope. Then, the staining was eluted with cetylpyridinium chloride (CPC) 10% (v/v) for 20 minutes with gentle agitation. Supernatants were collected and the mineralized calcium was quantified by measurement of absorbance at 570 nm. The concentration of calcium deposits in each sample was interpolated from an alizarin red standard curve.

Quantification of SAA3 and TNFα supernatant levels

SAA3 levels were quantified in supernatants recovered from BMDM and osteoclast cultures, using Mouse SAA-3 ELISA Kit (cat. no. EZMSAA3-12K, Millipore, USA), according to the manufacturer's instructions. The enzymatic activity was measured spectrophotometrically at 450 nm and corrected at 590 nm.

TNFα levels were quantified by Legend Max™ Mouse TNF-α ELISA Kit (cat. no. 430907, BioLegend®, USA) in the supernatants collected from BMDM cultures. The assay was performed according to the manufacturer's instructions. The enzymatic activity was measured at 450 nm and corrected at 570 nm.

RESULTS

Part of this section was presented in two national meetings: a poster communication at the 8th Molecular and Cell Biology Symposium, March 2022, Porto: O. Fonseca, T. Oliveira, MS. Gomes, AC. Gomes. "Production of Serum Amyloid A3 protein by *Mycobacterium avium*-infected macrophages drives osteoporosis during infection"; and an oral communication at IJUP'22 – 15º Encontro de Investigação Jovem da Universidade do Porto, May 2022, Porto: O. Fonseca, T. Oliveira, MS. Gomes, AC. Gomes. "Production of Serum Amyloid A3 protein by *Mycobacterium avium*-infected macrophages drives osteoporosis during infection".

Also, part of this section was included in an original article already submitted while this thesis was being written: Ana Cordeiro Gomes, Daniela Monteiro Sousa, Tiago Carvalho Oliveira, Óscar Fonseca, Ricardo J. Pinto, Diogo Silvério, Ana Fernandes, Ana Carolina Moreira, Tânia Silva, Maria José Teles, Graça Porto, Luísa Pereira, Margarida Saraiva, Meriem Lamghari, Maria Salomé Gomes. "Serum Amyloid A proteins reduce bone mass during mycobacterial infections" – Submitted.

Soluble molecules produced by infected macrophages enhance osteoclast activity, leading to increased bone resorption

To test whether soluble factors produced by *M. avium*-infected macrophages affected bone resorption, we studied osteoclastogenesis *in vitro* after supplementation with supernatants of BMDM cultures. For this purpose, bone marrow-derived macrophages were cultured, and conditioned media collected before (NI BMDM CM) and after (INF BMDM CM) 5 days of *M. avium* infection. Then, the conditioned media and saturating amounts of M-CSF and RANKL were added to bone marrow hematopoietic progenitors cultured on top of commercially available bovine bone slices. After 7 days of culture, the total numbers of pits and trenches as a readout of bone resorption were quantified. Macroscopically, we saw that the resorption events were far more abundant in the bone slices from osteoclasts cultured in the presence of INF BMDM CM (**Figure 8A, upper right panel**). We observed that the addition of INF BMDM CM increased, but not statistically significant, the total number of resorption events compared to the control condition (cells cultured only with M-CSF and RANKL) as well as NI BMDM CM (**Figure 8B**). Particularly, the proportion of trenches present in the INF BMDM CM condition compared to the control condition was 2:1 (**Figure 8B**).

Simultaneously, the direct effect of different cytokines was tested. IFNγ and TNFα were previously identified as important mediators of osteoclastogenesis during in vivo *M. avium* infection. Macroscopically, IFNγ addition did not seem to increase bone resorption compared to the control condition (**Figure 8A, lower left panel**). Indeed, the addition of IFNγ to the osteoclast cultures did not increase the number of pits and trenches formed, compared to the control condition (**Figure 8B**). On the other hand, TNFα enhanced the erosive activity of osteoclasts, as bone resorption events were augmented, although the results did not reach statistical significance (**Figure 8A, lower middle panel, and Figure 8B**). Of note, the total number of resorption events was similar between the cultures treated with TNFα and INF CM BMBM (**Figure 8B**). As we have previously observed that M-CSF was increased about 1.5-fold in the bone of infected mice (data not published), we increased M-CSF concentration in osteoclast cultures 1.5-fold to 150 ng/mL. We found that the augmented M-CSF concentration trend to increase the resorption events, compared to the control condition, (**Figure 8A, lower right panel, and Figure 8B**). Together, our data

indicate that soluble factors produced by infected macrophages and cytokines such as TNFα increase osteoclast activity, increasing bone resorption.

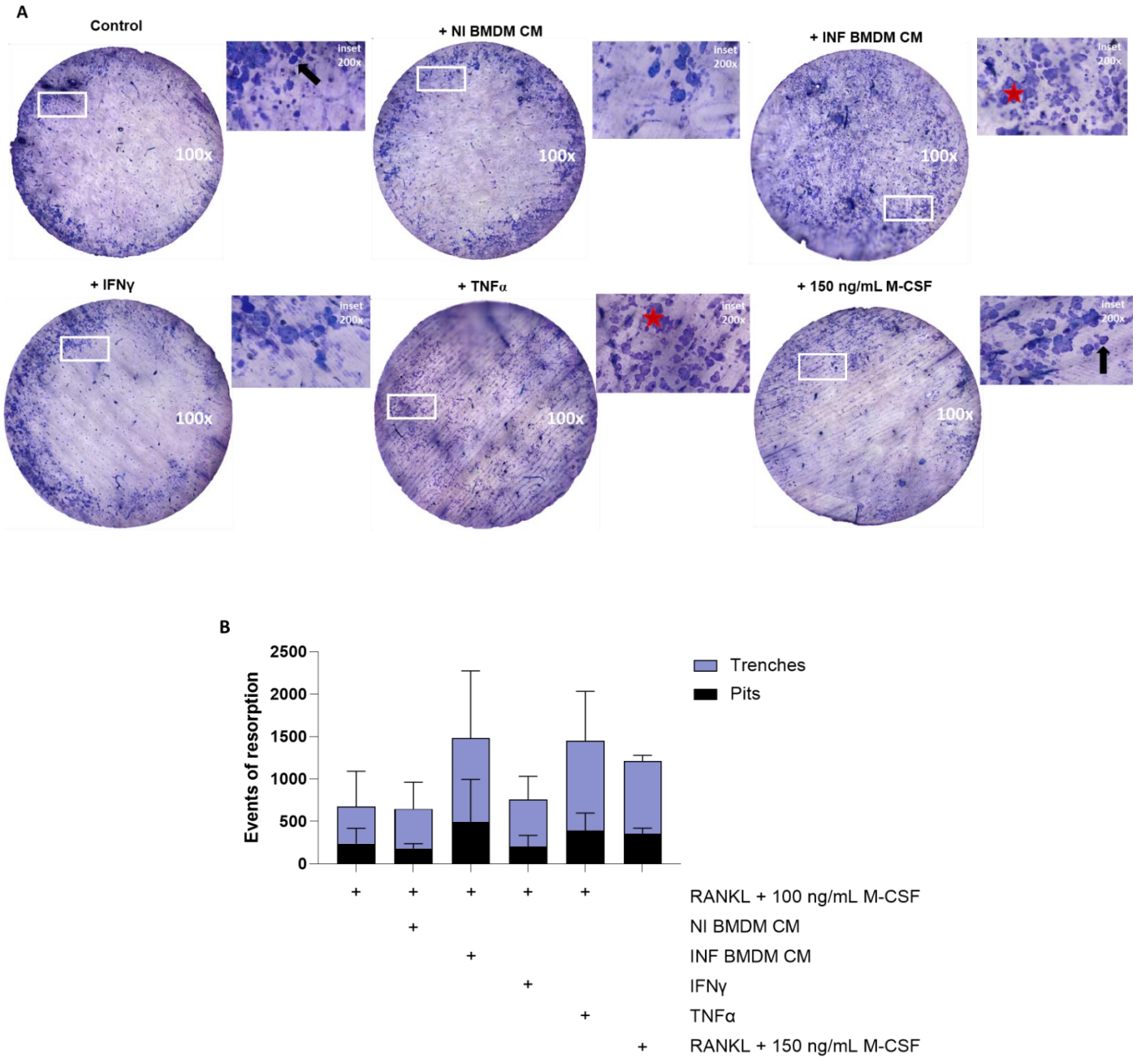

Figure 8 – Conditioned media from *M. avium*-infected bone marrow-derived macrophages and TNFα increase bone resorption *in vitro*. (**A**) Representative images of resorption events in bone slices in control condition (upper left panel), after supplementation with conditioned media from non-infected (upper middle panel) and infected (upper right panel) macrophages, with addition of IFNγ (lower left panel), TNFα (lower middle panel), or an increased concentration of M-CSF (lower right panel). Amplification: 100x. On the insets, examples of pits are labeled with black arrows and of trenches with red stars. Amplification: 200x. (**B**) Enumeration of pits (black bars) and trenches (purple bars). Data are representative of two independent experiments. Bars represent the mean ± standard deviation of each condition tested (n = 4).

During bone resorption, osteoclasts secrete TRAP, whose activity in the conditioned media of osteoclast cultures represents a readout of osteoclast-mediated bone resorption. The activity of TRAP was determined in the supernatants from the osteoclast cultures at different timepoints, using a colorimetric assay. We found that the activity of TRAP reached a maximum at day 6 of culture in all experimental conditions, except in the cultures supplemented with TNFα (whose peak activity was detected at day 4) (**Figure 9, red line**). The highest TRAP activity was observed in the supernatants containing BMDM CM and IFNγ, even though no statistically significant differences were found (**Figure 9, brown, gold, and green lines vs gray line**). TRAP activity decreased at day 7 of culture (**Figure 9**).

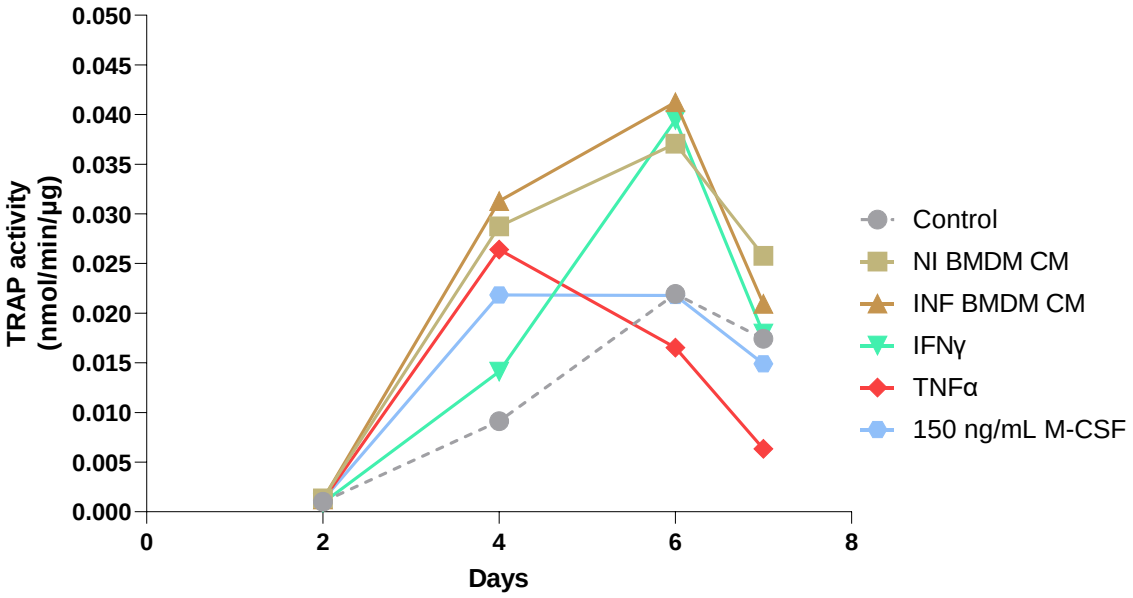

Figure 9 – Conditioned media from BMDM cultures increase TRAP activity. The graph represents the enzymatic kinetic of TRAP activity in nmol/min/µg during the 7 days of osteoclast culture. The activity was measured in the supernatants of all the tested conditions at days 2, 4, 6, and 7 of culture. Data are representative of two independent experiments. Each symbol represents the average of the experimental group at each timepoint. N=4 replicates per experimental group.

M. avium-infected macrophages upregulate SAA3 upon TNFα stimulation

INF BMDM CM and TNFα enhanced the resorptive activity of osteoclasts. Thus, we hypothesized that TNFα was one of the soluble factors produced by infected macrophages. To test our hypothesis, BMDM were cultured as described above and supplemented with 16 ng/mL IFNγ during the first 3 days post-infection (dpi). Then, TNFα levels were measured by ELISA in the conditioned media from the macrophages. TNFα concentration in the supernatants of non-infected macrophages was below the detection limit of the method (**Figure 10**). Furthermore, the conditioned media from *M. avium*-infected macrophages contained 3.4 ± 1.5 ρg/mL of TNFα, while infected macrophages supplemented with IFNγ produced 17.2 ± 3.6 ρg/mL of TNFα (**Figure 10**). These results indicate that TNFα is produced by infected macrophages, as it was expected. Moreover, the stimulation of BMDM with IFNγ led to a significant increase in the production of TNFα, with a concentration about five times higher than the one in which IFNγ was absent (**Figure 10**). Overall, the data indicated that IFNγ, a cytokine produced in response to mycobacterial infection, increases TNFα production by infected macrophages that in turn enhances osteoclast resorptive activity.

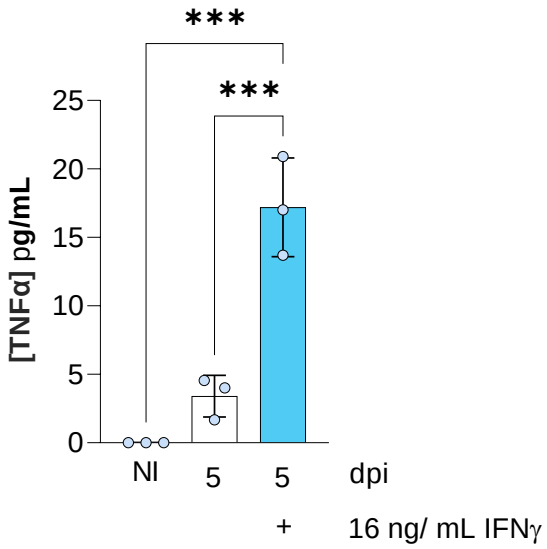

Figure 10 – *M. avium* infection and IFNγ increase the production of TNFα in bone marrow-derived macrophages. TNFα concentration in conditioned media from bone marrow-derived *M. avium*-infected macrophages supplemented with IFNγ. Concentration was assessed through an ELISA assay and expressed in ρg/mL. Bars represent the average ± standard deviation of the experimental group and dots represent each biological replicate. ***, $p<0.001$ by Two-way ANOVA.

Then, we questioned whether other soluble factors in the CM of INF BMDM play an important role in bone resorption. Targeted transcriptomic analysis of whole bones showed that the most upregulated gene in the bones of *M. avium*-infected mice was *Saa3*, which encodes for the Serum Amyloid A3 protein (data not published). Hence, we investigated *Saa3* expression in infected macrophages. We cultured and infected BMDM *in vitro* as described above. Then, 3 and 5 days post-infection, macrophages were lysed, RNA was extracted and *Saa3* expression was determined by qPCR. The expression of *Saa3* augmented 5 days post-infection (**Figure 11A**). Then, we tested the effect of IFNγ and TNFα stimulation on the expression of *Saa3*. Even though IFNγ did not enhance *Saa3* expression after infection, stimulation of infected macrophages with TNFα led to a 1500-fold upregulation of *Saa3* (**Figure 11A**), when compared to the control condition. Together, these results indicate that *M. avium* infection and TNFα enhance *Saa3* expression by macrophages. Furthermore, SAA3 levels in the CM of BMDM cultures were measured using a commercially available ELISA kit. SAA3 protein was detected in the conditioned media of infected macrophages (**Figure 11B, white bar**). Supplementation with IFNγ did not increase SAA3 production (**Figure 11B, blue bar**), as well as it did not significantly upregulate *Saa3* expression (**Figure 11A**). Likewise the gene expression, the levels of SAA3 increased in the supernatants of infected-macrophages stimulated with TNFα (**Figure 11B, red bar**).

As bone loss during *M. avium*-infection is TNFα dependent and *Saa3* is upregulated in the bone of infected mice (data not published), we determined *Saa3* expression in the bone of TNFα-deficient mice. The gene expression of *Saa3* in the bone of infected *Tnfalpha*$^{-/-}$ mice was similar to its expression in the bone of non-infected *Tnfalpha*$^{-/-}$ mice (**Figure 11C**), indicating that TNFα mediates the upregulation of *Saa3* during *M. avium* infection.

Then, we sought other cellular sources of SAA3 in the bone of infected mice. Osteoclasts and their progenitors are potential candidates [100]. For this purpose, SAA3 levels were measured in the supernatants of osteoclast cultures at different timepoints. The results indicated that in the presence of TNFα, SAA3 production by osteoclasts in culture was significantly augmented (**Figure 11D-F**).

Overall, our results indicate that *M. avium*-infected macrophages express and secrete SAA3, which is further enhanced by TNFα stimulation. Likewise, osteoclasts secrete SAA3 upon

TNFα stimulation. Furthermore, the expression of *Saa3 in vivo* during *M. avium* infection is modulated by TNFα.

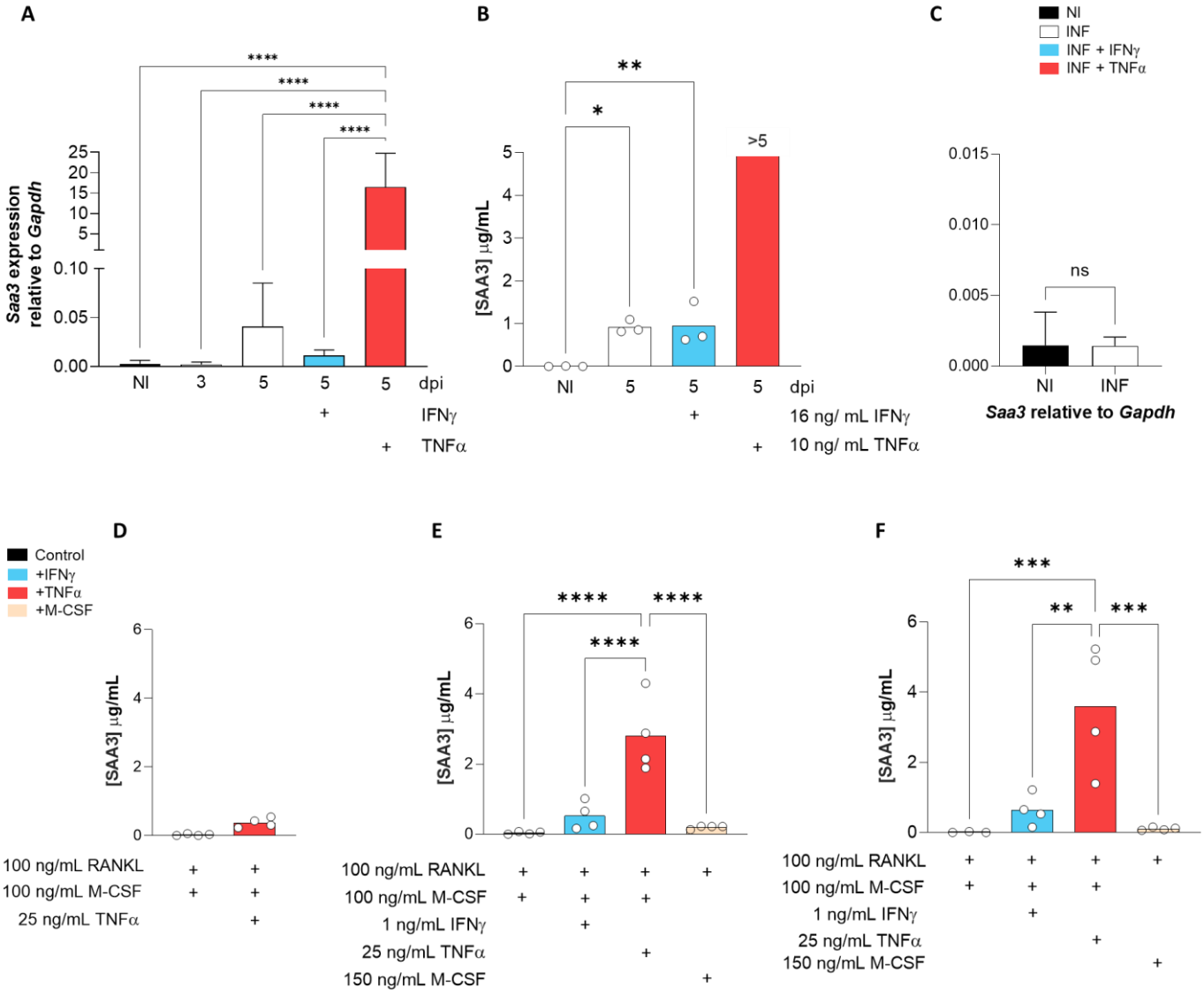

Figure 11 – *M. avium*-infection and TNFα enhance the expression and production of SAA3 by macrophages. (**A**) Saa3 expression relative to *Gapdh* in bone marrow-derived macrophages. Bars are representative of the average ± standard deviation of each analyzed group. (**B**) Quantification of SAA3 in BMDM culture supernatants. (**C**) Saa3 expression relative to *Gapdh* in the femurs of non-infected (black bar) and infected (white bar) *Tnfalpha*$^{-/-}$ mice. Bars indicate mean ± standard deviation. (**D-F**) Measurement of SAA3 protein levels in osteoclast cultures supernatants at days 2 (**D**), 4 (**E**), and 6 (**F**) of culture. Bars represent the mean of the experimental group and dots represent each biological replicate. *, p<0.05, ** p<0.01, ***, p<0.001, ****, p<0.0001, by Two-way ANOVA.

Human SAA protein induces the genesis of osteoclasts with more nuclei while not enhancing their resorptive activity

The direct role of SAA proteins in bone degradation was determined using morphological and functional studies. For morphological studies, osteoclasts were cultured in the presence of 5 µg/mL of recombinant Human Apo-SAA protein. At the 7th day of culture, cells were fixed, stained, and the formed osteoclasts were evaluated by fluorescence microscopy. The nuclei were labeled with DAPI and the cytoplasm with CellMask^{TM}. The addition of SAA led to the formation of multinucleated cells resembling osteoclasts that appeared significantly larger in size than the ones seen in the control condition (**Figure 12A**). For a more detailed study regarding osteoclast morphology, we divided the cells into four different ranges, according to their nuclei number: cells with 3 to 4 nuclei; cells with 5 to 10 nuclei; cells with 11 to 20 nuclei, and cells with more than 20 nuclei. The addition of SAA significantly decreased the number of cells with 3 to 4 nuclei, while significantly augmenting the frequency of the ones with more than 20 nuclei, compared with the cells without SAA stimulation (**Figure 12B**), suggesting that SAA enhances the formation of osteoclasts with an increased number of nuclei. For functional studies, osteoclasts were cultured on the top of bone slices, as described above. The addition of SAA to the osteoclast cultures slightly decreased the erosion of the bone surface, compared to the control condition (**Figure 12C**). Indeed, the supplementation of osteoclasts with SAA decreased the resorption activity of these cells, specifically the number of trenches (**Figure 12D**). Altogether, these results indicate that SAA leads to the formation of multinucleated cells resembling osteoclasts that have more nuclei but the higher number of nuclei per cell does not seem to associate with higher activity.

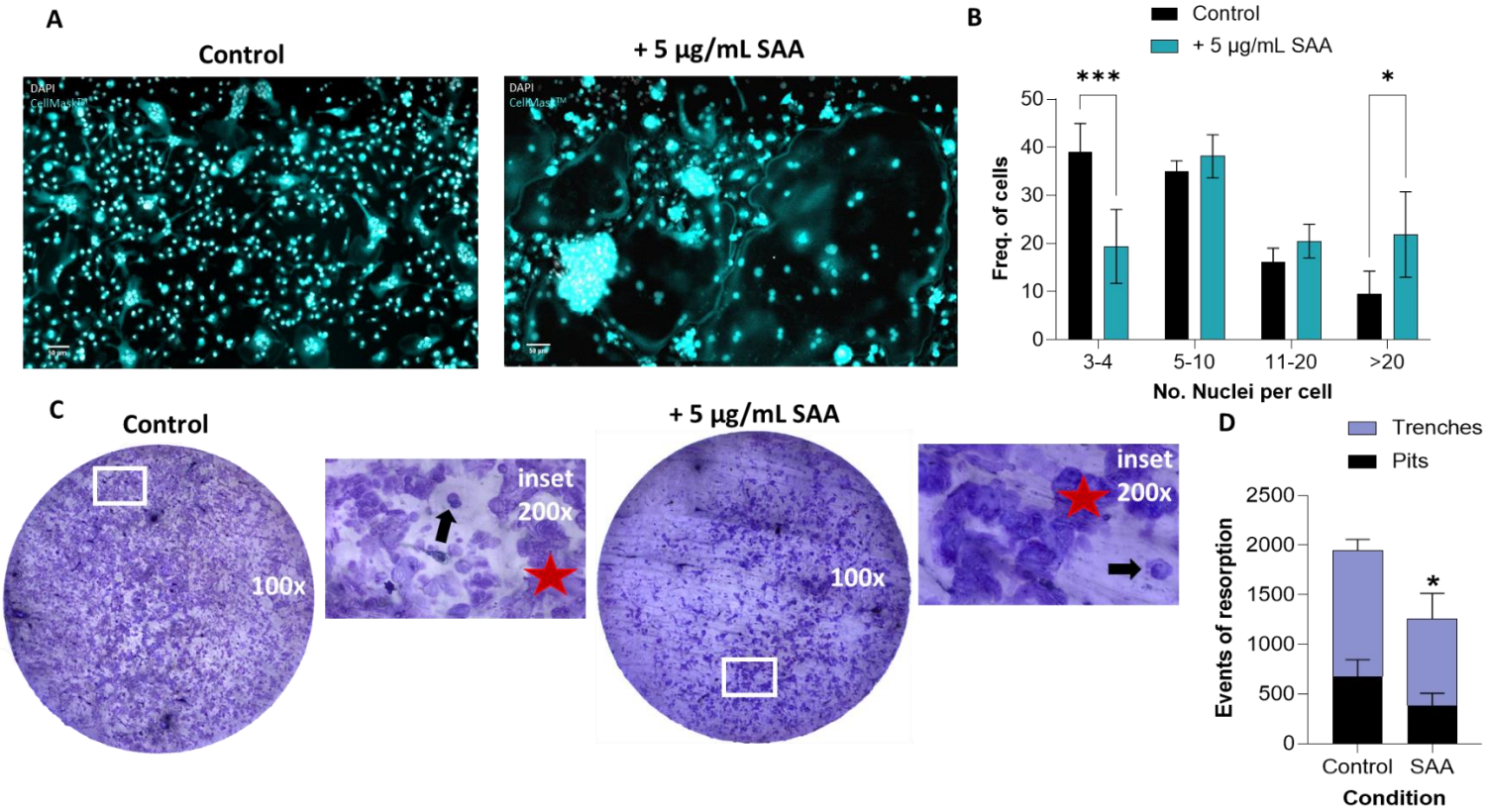

Figure 12 – SAA enhances osteoclastogenesis of larger multinucleated cells while not augmenting their resorptive capacity. (**A**) Representative microscope images of osteoclast cultures marked to nuclei (DAPI, in white) and cell cytoplasm (CellMask™, in cyan) in control condition (left panel) and supplemented with 5 µg/mL of recombinant Human Apo-SAA (right panel). Scale bar: 50 µm. (**B**) Quantification of multinucleated cells with more than 3 nuclei (osteoclasts) in each experimental condition (n=4 per condition). (**C**) Representative images of events of resorption in bone slices in control condition (left panel) and with supplementation with SAA (right panel). Amplification: 100x. On the insets, examples of pits are labeled with black arrows and of trenches with red stars. Amplification: 200x. (**D**) Enumeration of pits (black bars) and trenches (purple bars) (n=4 per condition). Data are representative of two independent experiments. *, $p<0.05$, ** $p<0.01$, ***, $p<0.001$, by Two-way ANOVA.

Thus far, our results show that SAA and TNFα are responsible for the increased osteoclast differentiation and resorptive activity. Thus, we tested the direct effects of the concerted action of SAA and TNFα in osteoclast cultures. We cultured osteoclasts as already described and supplemented them with 5 µg/mL of SAA and 25 ng/mL of TNFα and performed morphologic and functional assays as described above. Cultures with SAA and TNFα addition seem to form smaller cells with more nuclei, and a lot of cellular aggregates (**Figure 13A, right panel**), compared with the cultures without SAA and TNFα (**Figure 13A, left panel**). The addition of SAA and TNFα significantly decreased the frequency of cells with 3 to 4 nuclei and significantly increased the population of cells with 5 to 10 and 11 to 20

nuclei (**Figure 13B**). Fewer events of bone erosion were formed in the bone slices from the SAA and TNFα supplemented cultures, and a concomitant decrease in the formation of pits was observed, while the number of trenches remained practically the same (**Figure 13C**).

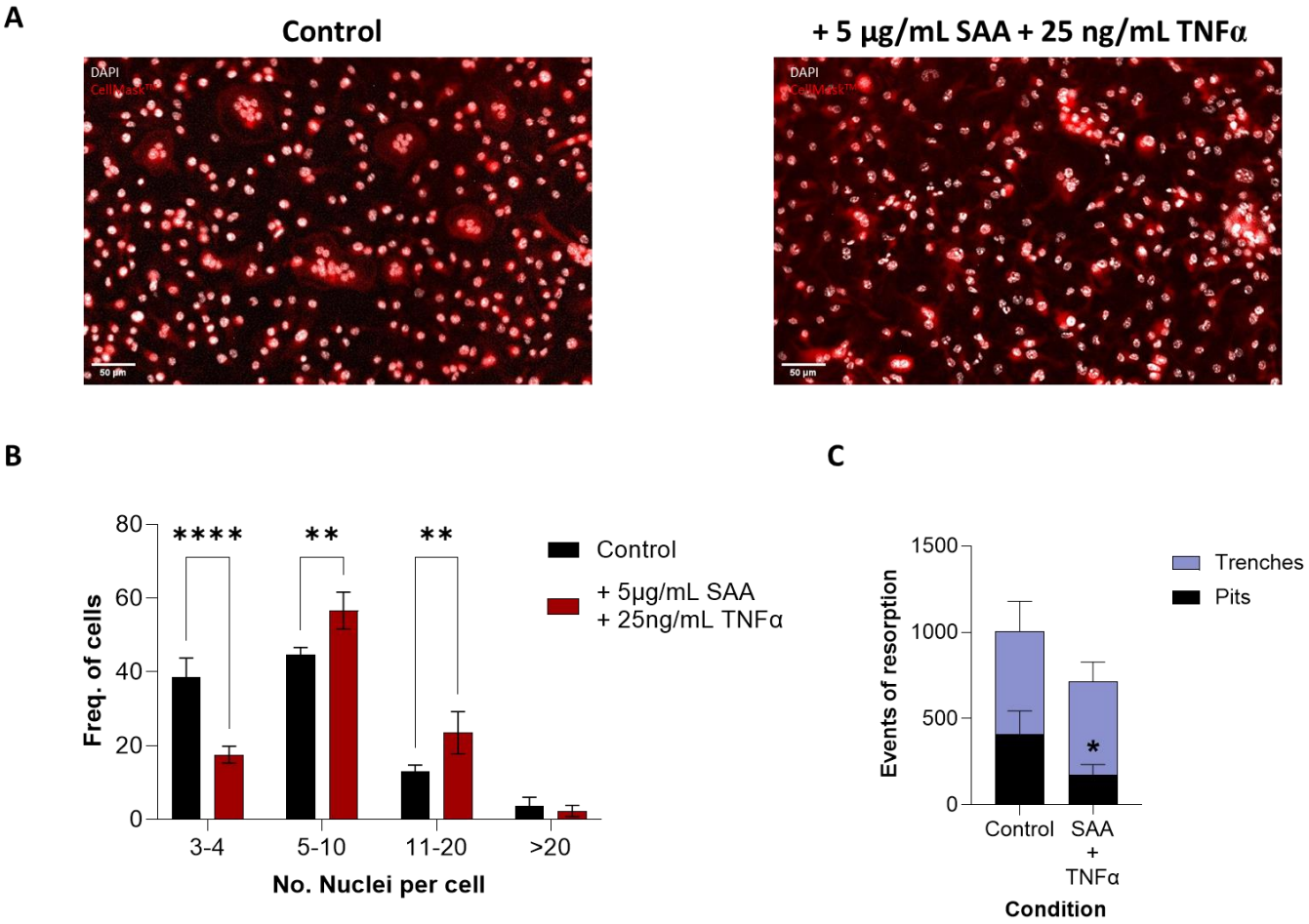

Figure 13 – SAA and TNFα form smaller osteoclasts with more nuclei, not enhancing their resorptive capacity. (**A**) Representative microscope images of osteoclast cultures labeled for nuclei (DAPI, in white) and cell cytoplasm (CellMask™, in red) in control condition (left panel) and in the presence of 5 µg/mL of recombinant Human Apo-SAA and 25 ng/mL of TNFα (right panel). Scale bar: 50 µm. (**B**) Frequency of osteoclasts (multinucleated cells with more than 3 nuclei) quantified in each experimental condition (n=4 per condition), grouped by number of nuclei per cell. (**C**) Count of resorption events in the pit mode (black bars) and in the trench mode (purple bars), in bone slices with osteoclasts supplemented or not with SAA and TNFα (n=4 per condition). *, p<0.05, ** p<0.01, ***, p<0.001, ****, p<0.0001, by Two-way ANOVA.

Bone formation *in vitro* is hampered by human SAA protein

Besides the increased bone degradation observed during *in vivo M. avium* infection, the mineral apposition rate was also decreased (data not published). Therefore, we hypothesized that *M. avium* infection, particularly infected macrophages, produce soluble factors that may interfere in the new bone formation process. To test this hypothesis, MSC were isolated from the bone marrow of non-infected B6 mice and osteoblast differentiation assays were performed *in vitro*. Along the assays, osteoblasts were supplemented or not with either 50% of conditioned media recovered from macrophage cultures infected and non-infected with *M. avium*, or with 5 µg/mL of human SAA protein. At the end of the differentiation assays, cells were fixed, and the bone matrix mineralization was detected by staining calcium deposits with alizarin red solution, further quantified by spectrophotometry. The addition of either infected or non-infected conditioned media from BMDM to the osteoblast cultures did not affect the deposition of mineralized calcium deposits (**Figure 14A-B**). Nevertheless, when the direct effect of human SAA protein was tested, the bone matrix mineralization was significantly reduced (**Figure 14C-D**). Altogether, these results indicate that the human SAA protein impairs new bone formation by impairing the development of new bone matrix.

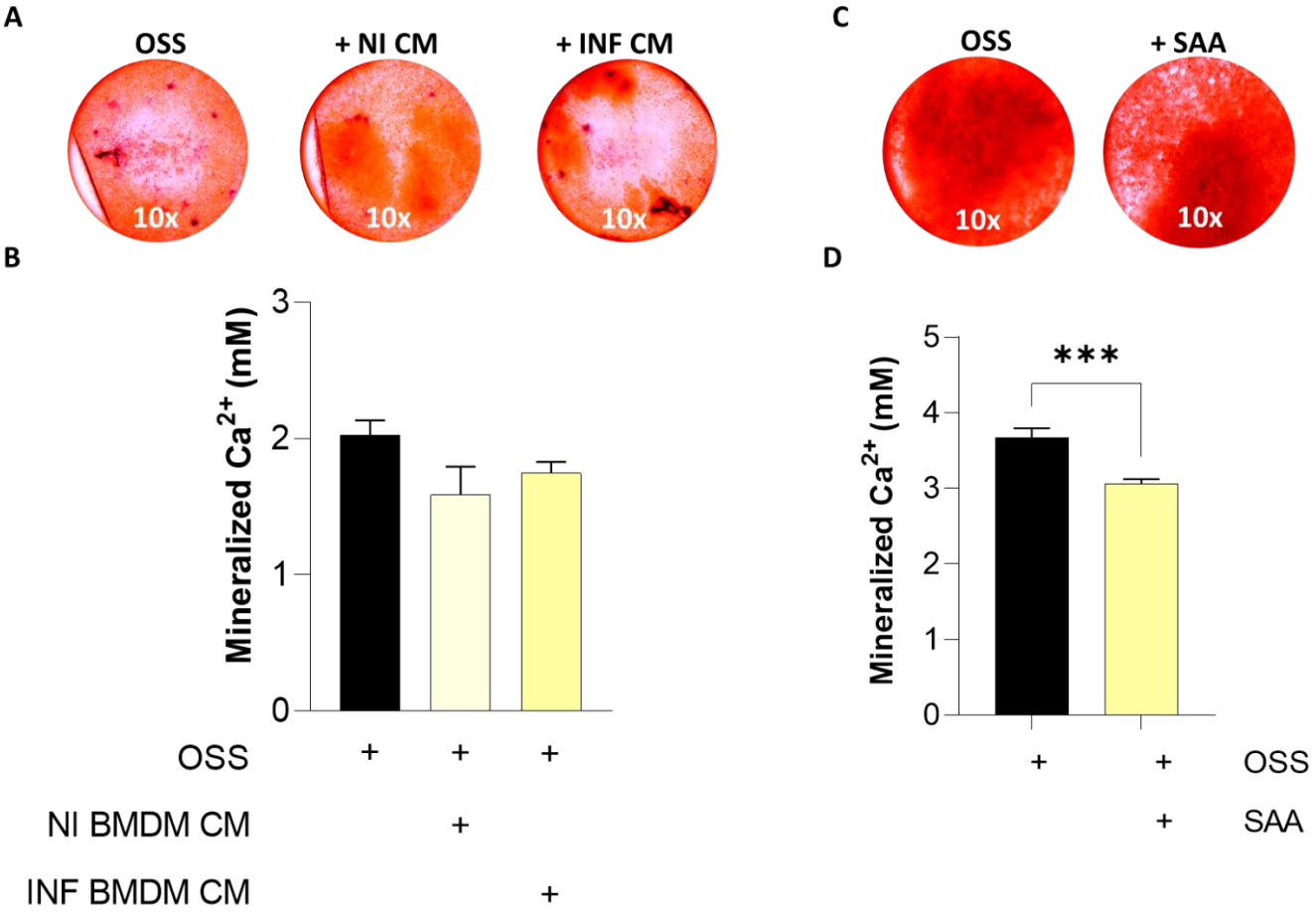

Figure 14 – Human SAA impairs new bone formation. (**A**) Representative images of murine osteoblast cultures with addition of osteoblast stimulatory supplement (OSS, left panel), plus NI BMDM CM (middle panel), and plus INF BMDM CM (right panel), stained with Alizarin Red. Amplification: 10x. (**B**) Quantification of deposited mineralized calcium. Bars represent the average ± standard deviation of each experimental condition (n=3 per condition). Data are representative of three independent experiments. (**C**) Representative images of murine osteoblast cultures with addition of osteoblast stimulatory supplement (OSS, left panel), and plus 5 µg/mL of human SAA protein (right panel), further stained with Alizarin Red. Amplification: 10x (**D**) Quantification of calcium deposits. Bars indicate the average ± standard deviation of 4 replicates per experimental group. *, $p<0.05$, ** $p<0.01$, ***, $p<0.001$ by Student's t test.

DISCUSSION

Bone loss during infection may arise from the dysregulation of either bone degradation or formation. Here, we show that *M. avium*-infected macrophages produce soluble pro-osteoclastogenic factors (SPOFs) that increase bone resorption by osteoclasts, which is also enhanced by TNFα and M-CSF. Additionally, we identified TNFα as one of those soluble factors. Moreover, TNFα production by infected macrophages is stimulated by IFNγ. Furthermore, we identified SAA3 as another SPOF produced by *M. avium*-infected macrophages and osteoclasts *in vitro,* and which production in the bone of *M. avium*-infected mice is TNFα-dependent *in vivo*. We also found evidence that SAA proteins stimulate the genesis of osteoclasts with more nuclei but less active in bone resorption. The addition of TNFα to osteoclast cultures stimulated with SAA enhanced the proportion of trenches, suggesting that the increased osteoclastogenesis and decreased bone mass *in vivo* are caused by the combined action of SAA and TNFα. We determined that the conditioned media from infected macrophages had no effect on the mineralization capacity of osteoblasts and that SAA diminished it, proving that SAA is a key player in the alterations of bone turnover.

Our lab's unpublished results have shown that the loss of bone mass in mice occurs during disseminated mycobacterial infection, without colonization of bone cells (data not published). Therefore, we aimed to discover the indirect molecular mechanism responsible for the pathophysiology of bone mass loss during chronic *M. avium* infection.

Firstly, we studied the effects of *M. avium* infection on the osteoclasts' capacity to degrade bone. Previously, we have found that during systemic infection, mycobacteria in the bone were mostly contained in macrophages within the bone marrow parenchyma [110], which led us to hypothesize that infected macrophages produce SPOFs that increase osteoclast activity. Additionally, we aimed to determine the effect of IFNγ, M-CSF, and TNFα on osteoclast activity, since we previously described how these factors altered osteoclast morphology concerning the number of nuclei per cell. Thus, we resorted to *in vitro* osteoclast resorption assays and the measurement of TRAP activity in the presence of INF or NI BMDM CM, IFNγ, M-CSF, or TNFα. Even though TRAP activity was not statistically different in the various experimental conditions, we found that the addition of conditioned media from infected macrophage cultures enhanced osteoclast activity. Importantly, we detected an increased proportion of the ratio trenches to pit events, suggesting that INF CM BMDM induces a more aggressive pattern of bone resorption, compared with the control condition. These results confirm our lab's previous observations that infected macrophages

produce soluble factors that enhance osteoclastogenesis. The addition of IFNγ, on the other hand, indicated that this cytokine did not enhance the resorptive activity of osteoclasts. This observation agrees with previous data from our lab regarding *in vitro* osteoclastogenesis studies, in which we found that IFNγ did not enhance the formation of osteoclasts. It has been described that IFNγ is directly anti-osteoclastogenic, as it inhibits osteoclast differentiation and leads to the apoptosis of osteoclasts [94]. However, the production of this cytokine is fundamental for the development of osteopenia in *M. avium*-infected mice (data not published). Therefore, it may be possible that IFNγ harnesses the macrophages to produce SPOFs that in turn affect bone degradation.

Our studies with M-CSF supplementation of osteoclast cultures trend to increase osteoclast erosive activity, correlating with our lab's previous unpublished results concerning osteoclast formation, which indicated that M-CSF led to the genesis of osteoclasts with more nuclei. Our lab's previous unpublished studies also showed that a 1.5-fold increase in the concentration of M-CSF (the same used in our resorption assays) led to similar alterations in the number of nuclei per osteoclast when compared to the effects of the addition of supernatants from infected-macrophages. Thus, it would be interesting to study the production of M-CSF at the gene expression and protein levels in *M. avium*-infected macrophages.

We also observed that TNFα increased the number of resorption events, thus indicating that osteoclast supplementation with this cytokine led to more active resorptive cells. TNFα affects bone degradation, as it enhances the proliferation of osteoclasts precursors [90], possibly leading to more erosive action. Curiously, our lab's previous results showed that TNFα supplementation enhanced the frequency of osteoclasts with fewer nuclei (data not published). Thus, our results suggest that less nucleated osteoclasts are more capable of resorbing bone, contradicting the usual dogma that correlates the number of nuclei with a higher resorptive activity [112]. However, supporting our observations, it was previously demonstrated that the formation of giant multinucleated osteoclasts does not correlate with an increased resorbing capacity [65]. Overall, we demonstrate that infected macrophages produce soluble factors that enhance the osteoclasts' ability to degrade bone, and perhaps TNFα is one of those.

To determine whether TNFα is a SPOF produced by infected macrophages, we cultured and infected BMDM *in vitro* and measured the TNFα concentration in the conditioned media of these cells. We determined that infected macrophages produced higher levels of TNFα, compared with the non-infected cells. As mentioned above, we observed that INF BMDM CM and TNFα had similar outcomes regarding bone degradation events. Thus, these results indicate that TNFα is a SPOF produced by *M. avium*-infected macrophages. Furthermore, we have demonstrated that IFNγ does not have a direct effect on bone resorption, although our lab's previous results have shown that IFNγ and TNFα are crucial for the development of osteopenia during *M. avium* infections (data not published). During *M. avium* infection, IFNγ instructs macrophages to augment TNFα production [113]. Our results confirmed that TNFα production by infected macrophages significantly increased with IFNγ supplementation. IFNγ and TNFα act in a concerted manner during mycobacterial infection [114]. Subsequent to its secretion by immune cells [42], IFNγ will act on infected macrophages to activate them and enhance their TNFα production. Although TNFα is produced to fight off the infection [42], we demonstrate that TNFα is also a SPOF, leading to bone loss, which is a collateral damage of the *M. avium* infection. However, we previously observed that TNFα action in osteoclastogenesis does not mimic the effects of INF BMDM CM in the number of nuclei per osteoclast (data not published), suggesting that there may exist other SPOFs produced by *M. avium*-infected macrophages.

Our previous data of transcriptomic analysis of whole bones from infected mice indicated that one of the most overexpressed genes was *Saa3* (data not published). Additionally, it has been already published by others that the *Saa3* gene is significantly upregulated in *M. tuberculosis*-infected BMDM [101] and that SAA induction may occur due to inflammatory stimuli like IFNγ or TNFα, among others [98]. Thus, we assessed whether SAA3 was a soluble factor secreted by *M. avium*-infected macrophages whose production was stimulated by IFNγ or TNFα. Firstly, we found that *M. avium* infection enhanced *Saa3* expression by macrophages and that TNFα significantly upregulated this gene, unlike IFNγ. Furthermore, we quantified SAA3 concentration in the supernatants from macrophage cultures. SAA3 production was significantly enhanced by infection, especially in the presence of TNFα, indicating that SAA3 is a soluble factor produced by *M. avium*-infected macrophages. Furthermore, our results indicate that TNFα acts as an autocrine factor in infected macrophages, stimulating them to produce SAA3. This observation is supported by others,

as it has been already demonstrated that TNFα may function in an autocrine manner to enhance macrophage activation following pathogen exposure [47]. We found that TNFα stimulation induces osteoclasts to produce SAA3 *in vitro*, which agrees with a previous observation that has shown that osteoclast precursors produce this protein [100]. Additionally, we also demonstrated that *Saa3* expression in the bone is dependent on TNFα production *in vivo*. Overall, SAA3 is produced by infected macrophages and osteoclasts, particularly in the presence of TNFα.

Then, we resorted to *in vitro* osteoclastogenesis studies in the presence of SAA to evaluate the direct role of this protein in osteoclast formation and activity. We found that osteoclast supplementation with SAA increased the number of cells with more than 20 nuclei while decreasing the frequency of the ones with 3 to 4 nuclei, forming apparently larger cells in size than the ones formed without SAA addition. We also performed resorption assays to assess the relation between the number of nuclei per osteoclast and their resorptive activity, and the results showed that osteoclasts supplemented with SAA were less active than the ones without this protein. Also, we verified that SAA addition significantly decreased the number of trenches formed on the surface of the bone slices, indicating that SAA reduces bone degradation. Our results are in accordance with a previous study demonstrating that SAA enhances osteoclastogenesis [96]. However, they indicate that it does not improve osteoclast activity.

As we demonstrated that INF BMDM CM contains SAA and TNFα, we determined the combined effect of TNFα and SAA in osteoclast cultures. The simultaneous stimulation of osteoclast cultures with TNFα and SAA led to the increased formation of cells with 5 to 10 and 11 to 20 nuclei, but to a decreased frequency of cells with 3 to 4 nuclei. Interestingly, we observed that the osteoclasts with combined stimulation appeared to be smaller in size than the ones supplemented with only SAA, and that cell aggregates were formed, resembling our lab's previous TNFα results. As we determined that TNFα enhanced osteoclast activity, particularly in the trench mode, and that SAA diminished erosive activity, especially in the trench resorption mode, we assessed the combined effect of these factors in bone resorption assays. The simultaneous stimulation of osteoclasts with SAA and TNFα resulted in an impairment of their ability to degrade bone in the form of pits, while the number of trenches events were not affected, further confirming the role of TNFα in bone resorption. As TNFα was added, the SAA protein was unable to impair the formation of

resorption events in the form of trenches, characteristic of a more aggressive pattern of bone destruction. Altogether, it seems like the SAA and TNFα combined action leads to the formation of smaller osteoclasts with more nuclei and more active in bone resorption. It would also be interesting to evaluate osteoclast morphology and activity in *Saa3*$^{-/-}$ mice systemically infected with *M. avium*. Moreover, bone turnover assays or histomorphology analysis could be performed to further understand how the infection could alter the bone mass in the absence of the SAA3 protein.

As already mentioned, the genesis of osteoclasts arises from the fusion of monocyte/macrophage lineage cells [53], and to perform bone resorption, osteoclasts migrate over the bone surface [68]. Recent studies have described a new class of bone cells, called osteomorphs [115]. In these studies, it has been proved that giant multinucleated osteoclasts may disassemble by fission and generate smaller cells, which are more motile and may still undergo fusion with other cells to form recycled and active osteoclasts. Osteomorphs have been found in the bone marrow and blood and seem to migrate more efficiently to bone resorption locals than osteoclasts, before reassembling into giant active cells [115]. These recent discoveries led us to hypothesize that the observed cell aggregates in the osteoclastogenesis studies may be formed by osteomorphs. As TNFα potentiates the resorption capacity of osteoclasts it also may enhance faster cell migration, requiring the fission of osteoclasts to osteomorphs, to resorb the largest area of bone possible and in the shortest time. Thus, it would be interesting to validate the existence of osteomorphs in further osteoclastogenesis assays. Single-cell RNA sequencing can be used for this purpose, as previous data have demonstrated that osteomorphs resulting from the fission of osteoclasts are transcriptionally different from osteoclasts and macrophages [115].

Given the evidence of increased bone degradation caused by soluble factors produced by *M. avium*-infected macrophages, we further investigated how the bone formation arm of bone turnover would be affected by infection. Thus, we performed *in vitro* osteoblast differentiation assays from MSC to quantify the mineralized calcium secreted by osteoblasts, after the addition of INF BMDM CM. The results indicated that the osteoblastic mineralization function was not altered after supplementation with conditioned media, suggesting that osteoblasts are not affected by the SPOFs produced by infected macrophages. Additionally, as we determined that SAA is one of the SPOFs produced during infection, osteoblastogenesis assays were performed in the presence of SAA to assess the effect of this

protein on bone formation. The results revealed that the human SAA significantly reduced the bone matrix mineralization, which suggests that there may be other unknown soluble molecules on the previously added conditioned media that could counteract the role of SAA in the osteoblastic mineralization function. SAA is produced by osteoblasts following induction by homocysteine and it enhances the expression of genes like *MMP13*, important in bone matrix remodeling [99]. Interestingly, others have demonstrated that the production of SAA proteins by osteoblast progenitors [96] or by preosteoclasts [100] led to the impairment of osteoblast differentiation. Thus, is possible that the observed decrease in bone matrix mineralization has arisen from an impairment of the osteoblastic differentiation. Indeed, our previous results of bone whole transcriptome and pathway-enrichment analysis showed that the pathways related to bone formation were significantly downregulated in the bones of *M. avium*-infected mice (data not published). Furthermore, we observed that the total number of osteoblasts in the bone surface of infected mice was decreased while the number of MCS was significantly higher in those animals (data not published). Of note, the decrease in the number of osteoblasts could be due to TNFα produced during mycobacterial infection, as this cytokine impairs osteoblast differentiation [92] and promote osteoblast apoptosis [93]. Moreover, SAA is known to hamper osteoblastic differentiation [96, 100]. As mentioned, others have demonstrated that in mice lacking the capacity to produce SAA3, continuous PTH administration stimulated osteoblast differentiation [104]. Continuous PTH secretion leads to increased bone resorption [73]. Thus, perhaps the decrease in the osteoblastic mineralization function is due to SAA3, as it impairs osteoblast development upon continuous PTH stimulation, further leading to increased bone loss. Altogether, these data suggest that SAA3 is partly responsible for the diminished capacity of osteoblasts to differentiate and deposit new bone matrix, far contributing to the observed osteopenia during chronic *M. avium* infection.

SAA3 is also expressed and produced by osteocytes, and this production inhibits osteoblast differentiation as well as enhances osteoclastogenesis [96]. Thus, it would be relevant to study the production and deposition of SAA3 by osteocytes using an *in vivo* animal model of chronic *M. avium* infection.

FINAL REMARKS AND FUTURE PERSPECTIVES

Our work highlights a molecular mechanism for bone loss during chronic infection in which IFNγ, TNFα, and SAA3 are the key molecules. *M. avium*-infected macrophages are activated by IFNγ produced in response to infection perhaps by lymphoid cells. This activation leads to the production of TNFα by these infected macrophages. TNFα activates the macrophages in an autocrine manner to express and produce SAA3. The chronic *M. avium* infection correlates with alterations in bone homeostasis. On the one hand, TNFα and SAA3 affect the process of bone degradation performed by osteoclasts, modifying these cells either morphologically or functionally, with SAA3 augmenting osteoclast differentiation and TNFα enhancing their resorptive activity. On the other hand, SAA3 is responsible for impairing new bone formation as it inhibits osteoblast differentiation from MSC and blocks new bone matrix mineralization (**Figure 15**).

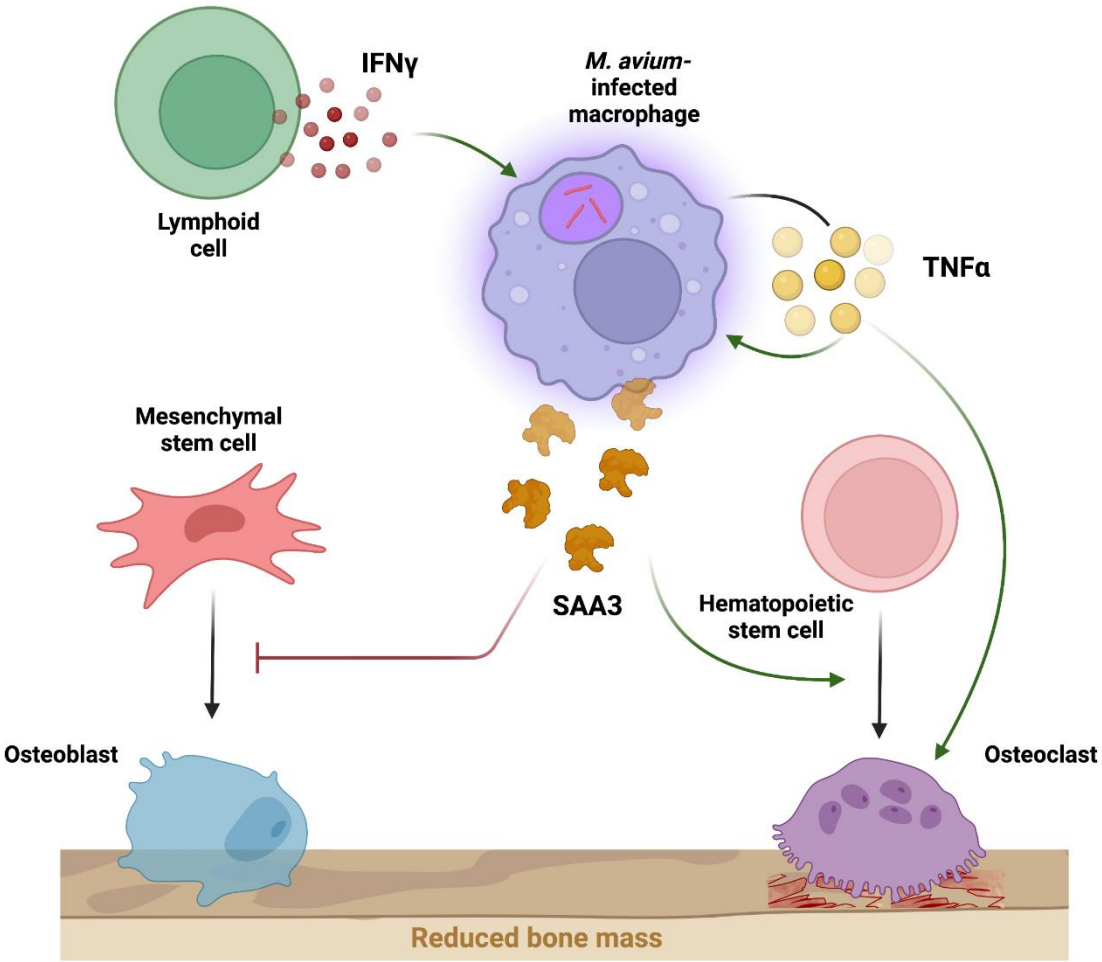

Figure 15 – Proposed molecular mechanism in which IFNγ, TNFα, and SAA3 reduce bone mass during chronic mycobacterial infection by enhancing bone degradation and impairing new bone formation. Figure created with BioRender.com.

In the future, it would be interesting to deepen our knowledge regarding other possible SPOFs produced by *M. avium*-infected macrophages. For this purpose, the supernatants recovered from the INF BMDM cultures could be extensively analyzed at a protein level, using proteomics techniques such as mass spectrometry. Furthermore, as M-CSF seemed to enhance the resorptive activity of osteoclasts, it would be relevant to assess if it is a SPOF by studying its production by infected macrophages at the gene expression and protein levels. Moreover, as the SAA3 protein proved itself to be of great importance in bone turnover, further experiments using *in vivo* mice models of *Saa3*$^{-/-}$ mice would be of interest. More specifically, bone histomorphology analysis, pit assays, and osteoclastogenesis studies should be addressed to determine how the absence of SAA3 affects the bone turnover. Additionally, systemic infection of those animals with *M. avium* would be helpful to clarify the importance of SAA3 in bone loss during chronic mycobacterial infection. Furthermore, *M. avium*-infected patients would be of great importance for further studies regarding SAA proteins. However, as *M. avium* infections have low incidence, patients infected with *M. tuberculosis* could be a viable alternative. Particularly, it would be interesting to find a correlation between SAA serum levels and bone loss in those patients, enabling the use of SAA proteins as biomarkers for bone loss during chronic mycobacterial infections.

REFERENCES

1. Jagielski, T., et al., *Methodological and Clinical Aspects of the Molecular Epidemiology of Mycobacterium tuberculosis and Other Mycobacteria.* Clin Microbiol Rev, 2016. **29**(2): p. 239-90.

2. Cook, G.M., et al., *Physiology of Mycobacteria*. 2009. p. 81-319.

3. Maitra, A., et al., *Cell wall peptidoglycan in Mycobacterium tuberculosis: An Achilles' heel for the TB-causing pathogen.* FEMS Microbiol Rev, 2019. **43**(5): p. 548-575.

4. Blanc, S.M., D. Robinson, and N.L. Fahrenfeld, *Potential for nontuberculous mycobacteria proliferation in natural and engineered water systems due to climate change: A literature review.* City and Environment Interactions, 2021. **11**: p. 100070.

5. Hett, E.C. and E.J. Rubin, *Bacterial growth and cell division: a mycobacterial perspective.* Microbiol Mol Biol Rev, 2008. **72**(1): p. 126-56.

6. Singh, B., et al., *Growth, cell division and sporulation in mycobacteria.* Antonie Van Leeuwenhoek, 2010. **98**(2): p. 165-77.

7. Klanicova-Zalewska, B. and I. Slana, *Presence and persistence of Mycobacterium avium and other nontuberculous mycobacteria in animal tissues and derived foods: a review.* Meat Sci, 2014. **98**(4): p. 835-41.

8. Smarda, P., et al., *Ecological and evolutionary significance of genomic GC content diversity in monocots.* Proc Natl Acad Sci U S A, 2014. **111**(39): p. E4096-102.

9. Vilchèze, C., et al., *Acid-Fast Positive and Acid-Fast Negative Mycobacterium tuberculosis: The Koch Paradox.* Microbiology Spectrum, 2017. **5**(2): p. 5.2.15.

10. Wanger, A., et al., *Biochemical Tests and Staining Techniques for Microbial Identification*, in *Microbiology and Molecular Diagnosis in Pathology*. 2017, Elsevier. p. 61-73.

11. Bayot, M.L., T.M. Mirza, and S. Sharma, *Acid Fast Bacteria*, in *StatPearls*. 2021: Treasure Island (FL).

12. Griffith, D.E., *Nontuberculous Mycobacterial Disease: An Introduction and Historical Perspective*, in *Nontuberculous Mycobacterial Disease: A Comprehensive Approach to Diagnosis and Management*, D.E. Griffith, Editor. 2019, Springer International Publishing: Cham. p. 1-14.

13. Khieu, V., et al., *Whole-Genome Sequencing Analysis to Identify Infection with Multiple Species of Nontuberculous Mycobacteria.* Pathogens, 2021. **10**(7): p. 879.

14. Alderwick, L.J., et al., *The Mycobacterial Cell Wall--Peptidoglycan and Arabinogalactan.* Cold Spring Harb Perspect Med, 2015. **5**(8): p. a021113.

15. Jankute, M., et al., *Assembly of the Mycobacterial Cell Wall.* Annu Rev Microbiol, 2015. **69**: p. 405-23.

16. Bento, C.M., M.S. Gomes, and T. Silva, *Looking beyond Typical Treatments for Atypical Mycobacteria.* Antibiotics (Basel), 2020. **9**(1): p. 18.

17. Vincent, A.T., et al., *The Mycobacterial Cell Envelope: A Relict From the Past or the Result of Recent Evolution?* Front Microbiol, 2018. **9**: p. 2341.

18. Abrahams, K.A. and G.S. Besra, *Mycobacterial cell wall biosynthesis: a multifaceted antibiotic target.* Parasitology, 2018. **145**(2): p. 116-133.

19. Johansen, M.D., J.L. Herrmann, and L. Kremer, *Non-tuberculous mycobacteria and the rise of Mycobacterium abscessus.* Nat Rev Microbiol, 2020. **18**(7): p. 392-407.

20. Franco-Paredes, C., et al., *Cutaneous Mycobacterial Infections.* Clinical Microbiology Reviews, 2018. **32**(1): p. e00069-18.

21. Botha, L., N.C. Gey van Pittius, and P.D. van Helden, *Mycobacteria and disease in southern Africa.* Transbound Emerg Dis, 2013. **60 Suppl 1**: p. 147-56.

22. WHO, *Global tuberculosis report* 2021, World Health Organization: Geneve, Switzerland.

23. WHO, *The End TB Strategy*. 2015, World Health Organization: Geneve, Switzerland.

24. Gopalaswamy, R., et al., *Of tuberculosis and non-tuberculous mycobacterial infections - a comparative analysis of epidemiology, diagnosis and treatment.* J Biomed Sci, 2020. **27**(1): p. 74.

25. Larsen, M.H., et al., *The Many Hosts of Mycobacteria 8 (MHM8): A conference report.* Tuberculosis (Edinb), 2020. **121**: p. 101914.

26. Lande, L., et al., *Association between pulmonary mycobacterium avium complex infection and lung cancer.* J Thorac Oncol, 2012. **7**(9): p. 1345-51.

27. Brode, S.K., C.L. Daley, and T.K. Marras, *The epidemiologic relationship between tuberculosis and non-tuberculous mycobacterial disease: a systematic review.* Int J Tuberc Lung Dis, 2014. **18**(11): p. 1370-7.

28. Hoefsloot, W., et al., *The geographic diversity of nontuberculous mycobacteria isolated from pulmonary samples: an NTM-NET collaborative study.* Eur Respir J, 2013. **42**(6): p. 1604-13.

29. Oliveira, M.J., et al., *Mycobacterium avium infection in Portugal.* Int J Tuberc Lung Dis, 2017. **21**(2): p. 218-222.

30. Busatto, C., et al., *Mycobacterium avium: an overview.* Tuberculosis (Edinb), 2019. **114**: p. 127-134.

31. Cosma, C.L., D.R. Sherman, and L. Ramakrishnan, *The secret lives of the pathogenic mycobacteria.* Annu Rev Microbiol, 2003. **57**: p. 641-76.

32. Cowman, S., et al., *Non-tuberculous mycobacterial pulmonary disease.* Eur Respir J, 2019. **54**.

33. Zahrt, Thomas C., *Molecular mechanisms regulating persistent Mycobacterium tuberculosis infection.* Microbes and Infection, 2003. **5**(2): p. 159-167.

34. Khan, A., et al., *Macrophage heterogeneity and plasticity in tuberculosis.* J Leukoc Biol, 2019. **106**(2): p. 275-282.

35. Prasla, Z., R.L. Sutliff, and R.T. Sadikot, *Macrophage Signaling Pathways in Pulmonary Nontuberculous Mycobacteria Infections.* Am J Respir Cell Mol Biol, 2020. **63**(2): p. 144-151.

36. Danelishvili, L., et al., *Mycobacterium avium subsp. hominissuis effector MAVA5_06970 promotes rapid apoptosis in secondary-infected macrophages during cell-to-cell spread.* Virulence, 2018. **9**(1): p. 1287-1300.

37. Appelberg, R., *Pathogenesis of Mycobacterium avium infection: typical responses to an atypical mycobacterium?* Immunol Res, 2006. **35**(3): p. 179-90.

38. Gomes, M.S., et al., *Survival of Mycobacterium avium and Mycobacterium tuberculosis in Acidified Vacuoles of Murine Macrophages.* Infection and Immunity, 1999. **67**(7): p. 3199-3206.

39. Guirado, E. and L.S. Schlesinger, *Modeling the Mycobacterium tuberculosis Granuloma - the Critical Battlefield in Host Immunity and Disease.* Front Immunol, 2013. **4**: p. 98.

40. Huynh, K.K., S.A. Joshi, and E.J. Brown, *A delicate dance: host response to mycobacteria.* Curr Opin Immunol, 2011. **23**(4): p. 464-72.

41. Bento, C.M., M.S. Gomes, and T. Silva, *Evolution of Antibacterial Drug Screening Methods: Current Prospects for Mycobacteria.* Microorganisms, 2021. **9**(12): p. 2562.

42. Cooper, A.M., K.D. Mayer-Barber, and A. Sher, *Role of innate cytokines in mycobacterial infection.* Mucosal Immunol, 2011. **4**(3): p. 252-60.

43. Torrado, E. and A.M. Cooper, *Cytokines in the balance of protection and pathology during mycobacterial infections.* Adv Exp Med Biol, 2013. **783**(1): p. 121-40.

44. Dorhoi, A. and S.H. Kaufmann, *Tumor necrosis factor alpha in mycobacterial infection.* Semin Immunol, 2014. **26**(3): p. 203-9.

45. Ghanavi, J., et al., *The role of interferon-gamma and interferon-gamma receptor in tuberculosis and nontuberculous mycobacterial infections.* Int J Mycobacteriol, 2021. **10**(4): p. 349-357.

46. Patel, S.Y., et al., *Anti-IFN-gamma autoantibodies in disseminated nontuberculous mycobacterial infections.* J Immunol, 2005. **175**(7): p. 4769-76.

47. Caldwell, A.B., et al., *Network dynamics determine the autocrine and paracrine signaling functions of TNF.* Genes Dev, 2014. **28**(19): p. 2120-33.

48. Adams, M.A., *Functional anatomy of the musculoskeletal system*, in *Gray's Anatomy: The Anatomical Basis of Clinical Practice*, S. Standrig, Editor. 2016, Elsevier: Amsterdam, The Netherlands. p. 84-96.

49. Feng, X. and J.M. McDonald, *Disorders of bone remodeling.* Annu Rev Pathol, 2011. **6**(1): p. 121-45.

50. Clarke, B., *Normal bone anatomy and physiology.* Clin J Am Soc Nephrol, 2008. **3 Suppl 3**: p. S131-9.

51. Oliveira, T.C., M.S. Gomes, and A.C. Gomes, *The Crossroads between Infection and Bone Loss.* Microorganisms, 2020. **8**(11): p. 1765.

52. Gomes, A.C., M. Saraiva, and M.S. Gomes, *The bone marrow hematopoietic niche and its adaptation to infection.* Semin Cell Dev Biol, 2021. **112**: p. 37-48.

53. Li, H., et al., *Osteoporosis: Mechanism, Molecular Target and Current Status on Drug Development.* Curr Med Chem, 2021. **28**(8): p. 1489-1507.

54. Komori, T., *Regulation of osteoblast differentiation by transcription factors.* J Cell Biochem, 2006. **99**(5): p. 1233-9.

55. Hill, T.P., et al., *Canonical Wnt/beta-catenin signaling prevents osteoblasts from differentiating into chondrocytes.* Dev Cell, 2005. **8**(5): p. 727-38.

56. Robling, A.G. and L.F. Bonewald, *The Osteocyte: New Insights.* Annu Rev Physiol, 2020. **82**(1): p. 485-506.

57. Joeng, K.S., et al., *Osteocyte-specific WNT1 regulates osteoblast function during bone homeostasis.* J Clin Invest, 2017. **127**(7): p. 2678-2688.

58. Bolamperti, S., I. Villa, and A. Rubinacci, *Bone remodeling: an operational process ensuring survival and bone mechanical competence.* Bone Res, 2022. **10**(1): p. 48.

59. Feng, W., J. Guo, and M. Li, *RANKL-independent modulation of osteoclastogenesis.* J Oral Biosci, 2019. **61**(1): p. 16-21.

60. Gruber, M.F. and T.L. Gerrard, *Production of macrophage colony-stimulating factor (M-CSF) by human monocytes is differentially regulated by GM-CSF, TNF alpha, and IFN-gamma.* Cell Immunol, 1992. **142**(2): p. 361-9.

61. Campbell, I.K., G. Ianches, and J.A. Hamilton, *Production of macrophage colony-stimulating factor (M-CSF) by human articular cartilage and chondrocytes. Modulation by interleukin-1 and tumor necrosis factor alpha.* Biochim Biophys Acta, 1993. **1182**(1): p. 57-63.

62. Dai, X.M., et al., *Targeted disruption of the mouse colony-stimulating factor 1 receptor gene results in osteopetrosis, mononuclear phagocyte deficiency, increased primitive progenitor cell frequencies, and reproductive defects.* Blood, 2002. **99**(1): p. 111-20.

63. Nevius, E., A.C. Gomes, and J.P. Pereira, *Inflammatory Cell Migration in Rheumatoid Arthritis: A Comprehensive Review.* Clin Rev Allergy Immunol, 2016. **51**(1): p. 59-78.

64. Kobayashi, K., et al., *Tumor necrosis factor alpha stimulates osteoclast differentiation by a mechanism independent of the ODF/RANKL-RANK interaction.* J Exp Med, 2000. **191**(2): p. 275-86.

65. Sousa, D.M., et al., *Ablation of Y1 receptor impairs osteoclast bone-resorbing activity.* Sci Rep, 2016. **6**: p. 33470.

66. Kim, J.M., et al., *Osteoblast-Osteoclast Communication and Bone Homeostasis.* Cells, 2020. **9**(9): p. 2073.

67. Borggaard, X.G., et al., *Osteoclasts' Ability to Generate Trenches Rather Than Pits Depends on High Levels of Active Cathepsin K and Efficient Clearance of Resorption Products.* Int J Mol Sci, 2020. **21**(16): p. 5924.

68. Merrild, D.M., et al., *Pit- and trench-forming osteoclasts: a distinction that matters.* Bone Res, 2015. **3**: p. 15032.

69. Soe, K. and J.M. Delaisse, *Time-lapse reveals that osteoclasts can move across the bone surface while resorbing.* J Cell Sci, 2017. **130**(12): p. 2026-2035.

70. Delaisse, J.M., et al., *The Mechanism Switching the Osteoclast From Short to Long Duration Bone Resorption.* Front Cell Dev Biol, 2021. **9**: p. 644503.

71. Gao, Y., S. Patil, and J. Jia, *The Development of Molecular Biology of Osteoporosis.* Int J Mol Sci, 2021. **22**(15): p. 8182.

72. Goltzman, D., *Physiology of Parathyroid Hormone.* Endocrinol Metab Clin North Am, 2018. **47**(4): p. 743-758.

73. Kraenzlin, M.E. and C. Meier, *Parathyroid hormone analogues in the treatment of osteoporosis.* Nat Rev Endocrinol, 2011. **7**(11): p. 647-56.

74. Nakamura, T., et al., *Estrogen prevents bone loss via estrogen receptor alpha and induction of Fas ligand in osteoclasts.* Cell, 2007. **130**(5): p. 811-23.

75. Delmas, P.D., *Treatment of postmenopausal osteoporosis.* The Lancet, 2002. **359**(9322): p. 2018-2026.

76. Karaguzel, G. and M.F. Holick, *Diagnosis and treatment of osteopenia.* Rev Endocr Metab Disord, 2010. **11**(4): p. 237-51.

77. Ensrud, K.E., *Epidemiology of fracture risk with advancing age.* J Gerontol A Biol Sci Med Sci, 2013. **68**(10): p. 1236-42.

78. Masters, E.A., et al., *Skeletal infections: microbial pathogenesis, immunity and clinical management.* Nat Rev Microbiol, 2022. **20**(7): p. 385-400.

79. Maffulli, N., et al., *The management of osteomyelitis in the adult.* Surgeon, 2016. **14**(6): p. 345-360.

80. Rao, N., B.H. Ziran, and B.A. Lipsky, *Treating osteomyelitis: antibiotics and surgery.* Plast Reconstr Surg, 2011. **127 Suppl 1**: p. 177S-187S.

81. Hogan, J.I., R.M. Hurtado, and S.B. Nelson, *Mycobacterial Musculoskeletal Infections.* Thorac Surg Clin, 2019. **29**(1): p. 85-94.

82. Bi, S., et al., *Nontuberculous mycobacterial osteomyelitis.* Infect Dis (Lond), 2015. **47**(10): p. 673-85.

83. Dym, H. and J. Zeidan, *Microbiology of Acute and Chronic Osteomyelitis and Antibiotic Treatment.* Dent Clin North Am, 2017. **61**(2): p. 271-282.

84. Redlich, K. and J.S. Smolen, *Inflammatory bone loss: pathogenesis and therapeutic intervention.* Nat Rev Drug Discov, 2012. **11**(3): p. 234-50.

85. Mundy, G.R., *Osteoporosis and Inflammation.* Nutrition Reviews, 2007. **65**(12): p. 147-151.

86. Liu, W., et al., *Mycobacterium tuberculosis infection increases the number of osteoclasts and inhibits osteoclast apoptosis by regulating TNF-alpha-mediated osteoclast autophagy.* Exp Ther Med, 2020. **20**(3): p. 1889-1898.

87. Yin, X., et al., *Autophagy in bone homeostasis and the onset of osteoporosis.* Bone Res, 2019. **7**: p. 28.

88. Kon, T., et al., *Expression of osteoprotegerin, receptor activator of NF-kappaB ligand (osteoprotegerin ligand) and related proinflammatory cytokines during fracture healing.* J Bone Miner Res, 2001. **16**(6): p. 1004-14.

89. Petrova, N.L., et al., *Inhibition of TNF-alpha Reverses the Pathological Resorption Pit Profile of Osteoclasts from Patients with Acute Charcot Osteoarthropathy.* J Diabetes Res, 2015. **2015**.

90. Yao, Z., et al., *Tumor necrosis factor-alpha increases circulating osteoclast precursor numbers by promoting their proliferation and differentiation in the bone marrow through up-regulation of c-Fms expression.* J Biol Chem, 2006. **281**(17): p. 11846-55.

91. Hess, K., et al., *TNFalpha promotes osteogenic differentiation of human mesenchymal stem cells by triggering the NF-kappaB signaling pathway.* Bone, 2009. **45**(2): p. 367-76.

92. Zhao, L., et al., *Tumor necrosis factor inhibits mesenchymal stem cell differentiation into osteoblasts via the ubiquitin E3 ligase Wwp1.* Stem Cells, 2011. **29**(10): p. 1601-10.

93. Zhang, S., et al., *Involvement of the TNF-alpha/SATB2 axis in the induced apoptosis and inhibited autophagy of osteoblasts by the antipsychotic Risperidone.* Mol Med, 2022. **28**(1): p. 46.

94. Tang, M., et al., *Interferon-Gamma-Mediated Osteoimmunology.* Front Immunol, 2018. **9**: p. 1508.

95. Gao, Y., et al., *IFN-gamma stimulates osteoclast formation and bone loss in vivo via antigen-driven T cell activation.* J Clin Invest, 2007. **117**(1): p. 122-32.

96. Thaler, R., et al., *Acute-phase protein serum amyloid A3 is a novel paracrine coupling factor that controls bone homeostasis.* FASEB J, 2015. **29**(4): p. 1344-59.

97. Soric Hosman, I., I. Kos, and L. Lamot, *Serum Amyloid A in Inflammatory Rheumatic Diseases: A Compendious Review of a Renowned Biomarker.* Front Immunol, 2020. **11**: p. 631299.

98. Sack, G.H., Jr., *Serum amyloid A - a review.* Mol Med, 2018. **24**(1): p. 46.

99. Thaler, R., et al., *Homocysteine induces serum amyloid A3 in osteoblasts via unlocking RGD-motifs in collagen.* FASEB J, 2013. **27**(2): p. 446-63.

100. Choudhary, S., et al., *Serum Amyloid A3 Secreted by Preosteoclasts Inhibits Parathyroid Hormone-stimulated cAMP Signaling in Murine Osteoblasts.* J Biol Chem, 2016. **291**(8): p. 3882-94.

101. Leisching, G., et al., *RNAseq reveals hypervirulence-specific host responses to M. tuberculosis infection.* Virulence, 2017. **8**(6): p. 848-858.

102. Dong, Y., et al., *P2X7 receptor acts as an efficient drug target in regulating bone metabolism system.* Biomed Pharmacother, 2020. **125**: p. 110010.

103. Choudhary, S., et al., *Prostaglandin E2 acts via bone marrow macrophages to block PTH-stimulated osteoblast differentiation in vitro.* Bone, 2013. **56**(1): p. 31-41.

104. Choudhary, S., et al., *Continuous PTH in Male Mice Causes Bone Loss Because It Induces Serum Amyloid A.* Endocrinology, 2018. **159**(7): p. 2759-2776.

105. Thorn, C.F., Z.Y. Lu, and A.S. Whitehead, *Tissue-specific regulation of the human acute-phase serum amyloid A genes, SAA1 and SAA2, by glucocorticoids in hepatic and epithelial cells.* Eur J Immunol, 2003. **33**(9): p. 2630-9.

106. Li, X., et al., *Clinical characteristics of 25 death cases with COVID-19: A retrospective review of medical records in a single medical center, Wuhan, China.* Int J Infect Dis, 2020. **94**: p. 128-132.

107. Mo, X.N., et al., *Serum amyloid A is a predictor for prognosis of COVID-19.* Respirology, 2020. **25**(7): p. 764-765.

108. Tanaka, H., et al., *Osteoporosis in nontuberculous mycobacterial pulmonary disease: a cross-sectional study.* BMC Pulm Med, 2022. **22**(1): p. 202.

109. Bastos, H.N., et al., *A Prediction Rule to Stratify Mortality Risk of Patients with Pulmonary Tuberculosis.* PLoS One, 2016. **11**(9): p. e0162797.

110. Gomes, A.C., et al., *IFN-gamma-Dependent Reduction of Erythrocyte Life Span Leads to Anemia during Mycobacterial Infection.* J Immunol, 2019. **203**(9): p. 2485-2496.

111. Lau, K.H., et al., *Characterization and assay of tartrate-resistant acid phosphatase activity in serum: potential use to assess bone resorption.* Clin Chem, 1987. **33**(4): p. 458-62.

112. Boissy, P., et al., *Transcriptional activity of nuclei in multinucleated osteoclasts and its modulation by calcitonin.* Endocrinology, 2002. **143**(5): p. 1913-21.

113. Appelberg, R., *Protective Role of Interferon Gamma, Tumor Necrosis Factor Alpha and Interleukin-6 in Mycobacterium tuberculosis and M. avium Infections.* Immunobiology, 1994. **191**(4-5): p. 520-525.

114. Appelberg, R., et al., *Role of gamma interferon and tumor necrosis factor alpha during T-cell-independent and -dependent phases of Mycobacterium avium infection.* Infect Immun, 1994. **62**(9): p. 3962-71.

115. McDonald, M.M., et al., *Osteoclasts recycle via osteomorphs during RANKL-stimulated bone resorption.* Cell, 2021. **184**(5): p. 1330-1347 e13.